and its advantage is obvious over simple spatial mapping of the expression profiles on chromosomal location. Therefore, the EIM would provide the user with further insight into the genomic structure through mRNA expression.

This work was supported by Grant-in-Aid for Scientific Research on Priority Areas (C) "Genome Information Science" from the Ministry of Education, Culture, Sports, Science and Technology of Japan.

REFERENCES

1. **Bhattacharjee A, Richards WG, Staunton J, Li C, Monti S, Vasa P, Ladd C, Beheshti J, Bueno R, Gillette M, Loda M, Weber G, Mark EJ, Lander ES, Wong W, Johnson BE, Golub TR, Sugarbaker DJ, and Meyerson M.** Classification of human lung carcinomas by mRNA expression profiling reveals distinct adenocarcinoma subclasses. *Proc Natl Acad Sci USA* 98: 13790–13795, 2001.
2. **Bonner RF, Emmert-Buck M, Cole K, Pohida T, Chuaqui R, Goldstein S, and Liotta LA.** Laser capture microdissection: molecular analysis of tissue. *Science* 278: 1481–1483, 1997.
3. **Fujii T, Dracheva T, Player A, Chacko S, Clifford R, Strausberg LS, Buetow K, Azumi N, Travis WD, and Jen J.** A preliminary transcriptome map of non-small cell lung cancer. *Cancer Res* 62: 3340–3346, 2002.
4. **Hayter AJ.** *Probability and Statistics for Engineers and Scientists* (2nd ed.). Florence, KY: Duxbury Press, 2002.
5. **Kallioniemi A, Kallioniemi OP, Sudar D, Rutovitz D, Gray JW, Waldman F, and Pinkel D.** Comparative genomic hybridization for molecular cytogenetic analysis of solid tumors. *Science* 258: 818–821, 1992.
6. **Lu YJ, Dong XY, Shipley J, Zhang RG, and Cheng SJ.** Chromosome 3 imbalances are the most frequent aberration found in non-small cell lung carcinoma. *Lung Cancer* 23: 61–66, 1999.
7. **Mukasa A, Ueki K, Matsumoto S, Tsutsumi S, Nishikawa R, Fujimaki T, Asai A, Kirino T, and Aburatani H.** Distinction in gene expression profiles of oligodendrogliomas with and without allelic loss of 1p. *Oncogene* 21: 3961–3968, 2002.
8. **Pei J, Balsara BR, Li W, Litwin S, Gabrielson E, Feder M, Jen J, and Testa JR.** Genomic imbalances in human lung adenocarcinomas and squamous cell carcinomas. *Genes Chromosomes Cancer* 31: 282–287, 2001.
9. **Petersen S, Aninat-Meyer M, Schluns K, Gellert K, Dietel M, and Petersen I.** Chromosomal alterations in the clonal evolution to the metastatic stage of squamous cell carcinomas of the lung. *Br J Cancer* 82: 65–73, 2000.
10. **Pollack JR, Perou CM, Alizadeh AA, Eisen MB, Pergamenschikov A, Williams CF, Jeffrey SS, Botstein D, and Brown PO.** Genome-wide analysis of DNA copy-number changes using cDNA microarrays. *Nat Genet* 23: 41–46, 1999.
11. **Reik W and Walter J.** Imprinting mechanisms in mammals. *Curr Opin Genet Dev* 8: 154–164, 1998.
12. **Virtaneva K, Wright FA, Tanner SM, Yuan B, Lemon WJ, Caligiuri MA, Bloomfield CD, de La Chapelle A, and Krahe R.** Expression profiling reveals fundamental biological differences in acute myeloid leukemia with isolated trisomy 8 and normal cytogenetics. *Proc Natl Acad Sci USA* 98: 1124–1129, 2001.

Physiol Genomics 15: 199–208, 2003.
First published September 9, 2003; 10.1152/physiolgenomics.00086.2003.

Identification of gene expression profile in tolerizing murine cardiac allograft by costimulatory blockade

Yuichi Matsui,[1,6] Akio Saiura,[1,6] Yasuhiko Sugawara,[1] Masataka Sata,[2] Katsutoshi Naruse,[1] Hideo Yagita,[3] Takahide Kohro,[6] Chikage Mataki,[6] Akashi Izumi,[6] Takuhiro Yamaguchi,[4] Takashi Minami,[6] Toshiko Sakihama,[6] Sigeo Ihara,[5] Hiroyuki Aburatani,[5] Takao Hamakubo,[6] Tatsuhiko Kodama,[6] and Masatoshi Makuuchi[1]

Departments of [1]Hepato-Biliary-Pancreatic and Transplantation Surgery and [2]Cardiovascular Medicine, Graduate School of Medicine, University of Tokyo, Tokyo 113-8655; [3]Department of Immunology, Juntendo University School of Medicine, Tokyo 113-8421; [4]Biostatistics/ Epidemiology and Preventive Health Sciences, School of Health Sciences and Nursing, University of Tokyo, Tokyo 113-8655; and [5]Genome Sciences and [6]Department of Molecular Biology and Medicine, Research Center for Advanced Science and Technology, University of Tokyo, Tokyo 153-8904, Japan

Submitted 19 May 2003; accepted in final form 27 August 2003

Matsui, Yuichi, Akio Saiura, Yasuhiko Sugawara, Masataka Sata, Katsutoshi Naruse, Hideo Yagita, Takahide Kohro, Chikage Mataki, Akashi Izumi, Takuhiro Yamaguchi, Takashi Minami, Toshiko Sakihama, Sigeo Ihara, Hiroyuki Aburatani, Takao Hamakubo, Tatsuhiko Kodama, and Masatoshi Makuuchi. Identification of gene expression profile in tolerizing murine cardiac allograft by costimulatory blockade. *Physiol Genomics* 15: 199–208, 2003. First published September 9, 2003; 10.1152/physiolgenomics.00086.2003.—The induction of specific tolerance would be the ultimate achievement in transplant immunology, but the precise mechanisms of immunologic tolerance remain largely unknown. Here, we investigated global gene expression analysis in tolerizing murine cardiac allografts by means of oligonucleotide microarrays. Tolerance induction was achieved in cardiac allografts from BALB/c to C57BL/6 mice by daily intraperitoneal injection of anti-CD80 and anti-CD86 monoclonal antibodies (mAbs). Comparative analysis revealed 64 genes to be induced more extensively in the tolerizing than in the syngeneic isografts, and 16 genes than in the rejecting allografts. Two genes were specifically upregulated in the tolerizing allografts. In the tolerizing allografts there were induced marked expressions of a number of genes for pro-inflammatory factors, including interferon-γ-inducible cytokines and chemokines, as well as apoptosis-related genes, which were also upregulated in the rejecting allografts. Moreover, these gene expression patterns continued to be upregulated more than 70 days posttransplant. These results provide evidence that immunologic tolerance can be induced and maintained in the presence of prominent pro-inflammatory gene expression in vivo.

transplantation; immunologic tolerance; interferon-γ; chemokine; DNA microarray

ALTHOUGH RECENT ADVANCES in immunosuppressive therapy have dramatically enhanced the early survival of cardiac transplant recipients, acute rejection still occurs in ~50% of the recipients (21). Long-term immunosuppressive drug administration, furthermore, entails a number of potentially significant problems such as infection, spontaneous neoplasm, undesirable metabolic effects and drug toxicity. Alloantigen-specific tolerance induction is the ultimate goal in transplant immunology, and can be induced in a rodent model; however, the precise mechanisms by which specific tolerance is affected are not clearly understood, and the current immunosuppression regimens have all failed to achieve this goal in a clinical setting.

The mechanisms of allograft tolerance have been classified into categories of central and peripheral tolerance (14). Peripheral tolerance can be induced by the blockade of the T cell costimulatory pathway (11). Recent studies have demonstrated that activation-induced cell death of T cells is required for tolerance induction (22). Interleukin-2 (IL-2) and interferon-γ (IFN-γ) promote activation-induced cell death (13, 22). Consequently, IL-2-deficient and/or IFN-γ-deficient mice are resistant to tolerance induction (22). However, although there are increasing reported data describing the molecular mechanisms of tolerance induction, no systematic analysis has been carried out.

DNA microarray technology has made it possible to analyze the expression of a large number of genes and revolutionized many areas of biology and medicine (4). This new technology can provide nonbiased, global expressions of tens of thousands of genes simultaneously. Recent studies on gene expression profiles in various cardiac diseases, including cardiac allograft rejection, have successfully provided important information and new insights into the biological mechanisms of these diseases (23). The precise molecular mechanism of immunologic tolerance, however, has been relatively poorly dissected by comparison.

Here we provide a gene expression profile of the tolerizing allografts after costimulatory signal blockade in a murine cardiac transplant model. We also demonstrate vigorous gene expressions of pro-inflam-

Article published online before print. See web site for date of publication (http://physiolgenomics.physiology.org).

Address for reprint requests and other correspondence: T. Kodama, Dept. of System Molecular Biology, RCAST, Univ. of Tokyo, 4-6-1, Komaba, Meguro-ku, Tokyo 153-8904, Japan (E-mail: kodama@lsbm.org).

matory cytokines and chemokines, apoptosis, and signal transduction in the tolerizing cardiac allografts in vivo.

METHODS

Mice. Male BALB/c (H-2d) and C57BL/6 (H-2b) mice were purchased from Clea Japan (Tokyo, Japan). Adult males 6–8 wk of age were used throughout the study. All mice were kept in microisolator cages on a 12:12-h day/night cycle and fed on regular chow. All procedures involving experimental animals were carried out in accordance with protocols approved in the local institutional guideline for animal care of The University of Tokyo and complied with the "*Guide for the Care and Use of Laboratory Animals*" (NIH publication No. 86-23, revised 1985).

Monoclonal antibodies. Hybridomas producing anti-B7-1 and anti-B7-2 monoclonal antibodies (mAbs 1G10 and GL1, respectively) were kind gifts from Dr. Yagita of Juntendo University.

Heterotopic cardiac transplant. Cardiac transplants were performed according to the method of Corry and coworkers (6). In brief, donors and recipients were anesthetized intraperitoneally prior to surgery with 4% chloral hydrate at 0.01 ml/g body wt. Donor hearts were perfused with chilled, heparinized saline via the inferior vena cava. The aorta and pulmonary artery of the donor hearts were anastomosed to the abdominal aorta and inferior vena cava of the recipients by means of a microsurgical technique. The viability of the cardiac allografts was assessed by daily transabdominal palpation and confirmed by observation at laparotomy. Rejection of cardiac grafts was considered complete by the cessation of impulses and confirmed visually after laparotomy. Some recipients were injected intraperitoneally with 100 μg each of anti-CD80 and anti-CD86 mAbs daily for 5 days after transplantation (2).

Histological examination. Heart allografts and isografts were removed from the recipients under anesthesia with 4% chloral hydrate on *day 7* posttransplant. The graft was cut transversely into two sections, and the basal portion was fixed in 4% paraformaldehyde with the other section snap frozen for RNA extraction. The section at the edge of the maximal circumference was stained with hematoxylin and eosin.

Oligonucleotide microarray. After heterotopic cardiac transplantation, transplanted hearts were excised from the recipients and snap frozen in liquid nitrogen and stored at −80°C until use. Total RNA was then isolated independently using Isogen (Nippon Gene, Tokyo, Japan) according to the manufacturer's protocol. The quality of extracted total RNA was confirmed with an Agilent 2100 Bioanalyzer (Palo Alto, CA) or electrophoresis on 1.5% agarose gels stained by SYBR Green (Applied Biosystems, Foster City, CA).

Double-stranded complementary DNA was synthesized from 10 μg of total RNA according to Affymetrix (Affymetrix, Santa Clara, CA) methodology, and cDNA was purified with Phase Lock Gels (Eppendorf, Hamburg, Germany). We synthesized biotin-labeled RNA with the BioArray High Yield RNA Transcript Labeling Kit (Enzo, New York, NY).

Hybridization from biotinylated cRNA to murine genome GeneChips (MG-U74Av2, Affymetrix) was performed in accordance with the manufacturer's instructions, stored at 40°C overnight, heating in a mix that included 10 μg fragmented RNA, 6× SSPE, 0.005% Triton X-100, and 100 mg/ml herring sperm DNA in a total volume of 200 μl.

GeneChips were washed and stained with streptavidin-c (Molecular Probes, Eugene, OR), and probe arrays were scanned three times at 3-μm resolution using the GeneChip system confocal scanner made for Affymetrix by Hewlett-Packard.

MicroArray Suite (MAS) version 5.1 (Affymetrix) was utilized to calculate from the scanned images *1*) average difference, *2*) log ratio (base 2), and *3*) absolute call. Intensity values were scaled such that the overall intensity for each GeneChip of the same type was equivalent (4). The average difference of each experiment was normalized to 100 to allow comparison among multiple arrays.

To determine the absolute call (detected or not detected) of a specific probe set, the number of instances in which the perfect match (PM) hybridization signal was greater than the mismatch (MM) signal was computed by MAS ver. 5.1 (Affymetrix), along with the average of the logarithm of the PM/MM ratios for each probe set.

GEO accession numbers. Array data were deposited at the Gene Expression Omnibus (GEO) database of the National Center for Biotechnology Information with accession numbers GSM8926 through GSM8939. The array data are also available in series with accession number GSE582.

Data analysis. The gene expression profile consisted of the following three groups: *group A*, syngeneic isograft (C57BL/6 to C57BL/6); *group B*, rejecting allograft (BALB/c to C57BL/6); and *group C*, tolerizing allograft (BALB/c to C57BL/6 with daily intraperitoneal injection of anti-CD80 and anti-CD86 mAbs for 5 days after transplantation). Time course data was also collected on *day 7* ($n = 1$), *day 7* ($n = 3$), *day 28* ($n = 2$, *group C*) and *day 70* ($n = 2$, *group A*; $n = 3$, *group C*) after transplantation.

We compared the microarray data derived from the nine samples of the transplanted hearts excised on *day 7*. Analyses were performed based on the average difference, log ratio (base 2), and absolute call (presence or absence) for each gene among the triplicate samples of each group (Fig. 1). First, to exclude obscuring noise, all 12,488 probes on the MG-U74Av2 array were filtered by the average difference and absolute call (present or absent). The threshold values of an average difference of more than 50 in all three samples of the objective group, and at least one present call from among three in the group, were considered reliable for genes with expression values significantly over background. Second, we compared the log ratios (base 2), calculated by MAS 5.1 (Affymetrix). The threshold values of log ratio (base 2) of more than 1.58 (nearly equal to 3.0-fold) were considered reliable for genes upregulated significantly over baseline expression. Finally, singled-out genes were analyzed statistically with one-sided *t*-test and adjusted by means of a permutation-style resampling method using SAS version 8.2 (SAS/MULTTEST, SAS Institute) with significance set at $P \leq 0.05$ to control for the false-positive error rate associated with multiple tests. As for those genes screened out by these analyses, the time course data on *days 5*, *28*, and *70* after transplantation were also compared.

We used the computer program GeneSpring version 4.0 (Silicon Genetics, Redwood City, CA) to construct hierarchical clustering. Similarity was measured by standard correlation of the average difference for each gene, which was normalized to itself by making a synthetic positive control for that gene and dividing all measurements for that gene by this positive control, assuming it was at least 1.0. This synthetic control was the median of the gene's expression values over all the samples. Data are presented in a matrix format. Each row represents a single gene, and each column an experimental sample. The ratio of the abundance of transcripts of each gene to the median abundance of the gene's transcript is represented by a color in the corresponding sample in the matrix. Green squares indicate transcript

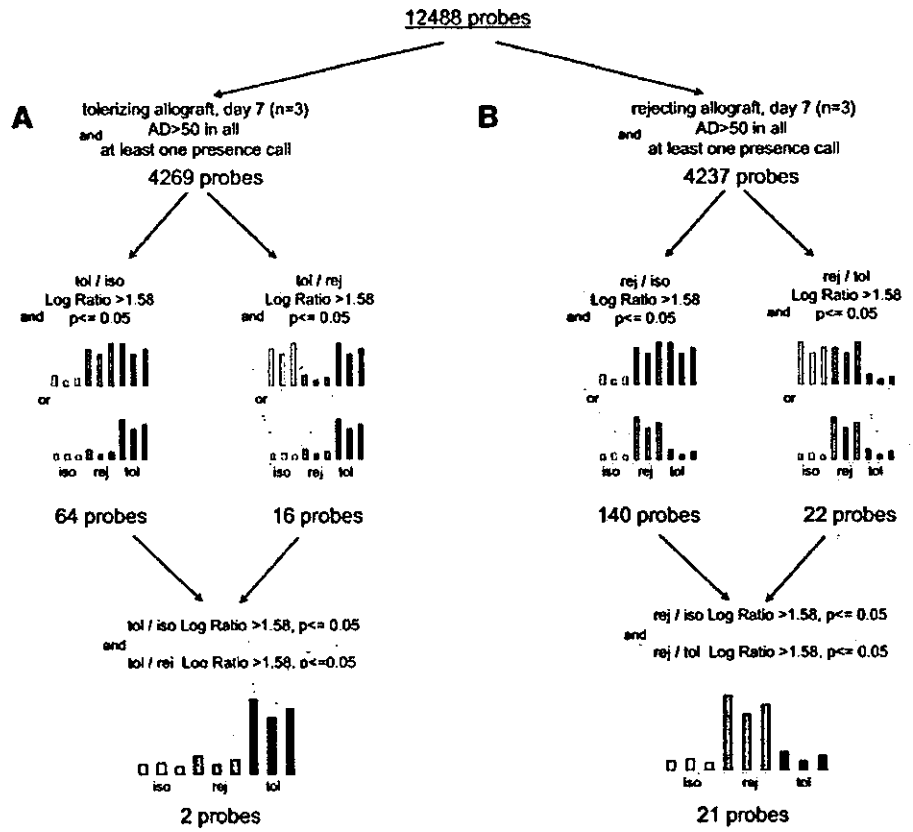

Fig. 1. Algorithm of the analyses used to identify genes induced specifically in the tolerizing (*A*) and rejecting (*B*) cardiac allografts. *A*: first, 12,488 probes on the MG-U74Av2 array were filtered in terms of average difference and present call to exclude noise. The threshold values of an average difference of more than 50 in all 3 samples and at least 1 present call from among 3 of the tolerizing cardiac allografts excised on *day 7* were considered reliable for genes with expression values significantly over background. As a result, 4,269 probes were left. Second, we compared the two log ratios of *1*) tolerizing allografts vs. syngeneic isografts and *2*) tolerizing allografts vs. rejecting allografts calculated by MAS 5.1 algorithm (Affymetrix). The threshold values of log ratio of more than 1.58 (nearly equal to 3.0-fold) were considered reliable for genes upregulated significantly over baseline expression. A total of 80 genes were more extensively expressed in tolerizing cardiac allografts than in syngeneic isografts and were analyzed statistically with one-sided *t*-test and adjusted by means of a permutation-style resampling method using SAS version 8.2 (SAS/MULTTEST) (SAS Institute). A total of 64 genes or expressed sequences tags (ESTs) were expressed statistically ($P \leq 0.05$) more extensively in the tolerizing allografts than in the syngeneic isografts. The same analysis performed on tolerizing vs. rejecting allografts revealed 16 genes were induced more in the tolerizing than in the rejecting allografts. Genes identified commonly in both analyses were considered to be genes upregulated specifically in tolerizing allografts. *B*: the same algorithm was applied to identify genes specifically induced in the rejecting cardiac allografts, which revealed 21 genes. tol, tolerizing cardiac allografts; iso, syngeneic cardiac isografts; rej, rejecting cardiac allografts; *P* value was calculated by SAS/MULTTEST (SAS Institute).

levels below the median; red squares indicate transcripts levels above the median; and white shadow signifies a lack of trust in the data.

Quantitative RT-PCR. To confirm the microarray data, quantitative real-time PCR was performed in an iCycler (Bio-Rad, Hercules, CA) using a SYBR Green PCR kit from Applied Biosystems and specific primers to amplify 100-200-bp fragments from the different genes analyzed. A threshold was set in the linear part of the amplification curve, and the number of cycles needed to reach the threshold was calculated for every gene. Normalization was achieved by including a sample with primers for hypoxanthine guanine phosphoribosyl transferase (HPRT) as a control.

To synthesize single-stranded cDNA, 1 μg of total RNA isolated from transplanted hearts on *days 7* and *70* ($n = 6$, respectively; distinct from the samples used for microarray analysis) was reverse transcribed using SuperScript II reverse transcriptase and an oligo$(dT)_{12-18}$ primer (Invitrogen Japan, Tokyo, Japan) in a final volume of 20 μl and diluted up to 80 μl.

PCR was then performed with 1 μl of cDNA for 1 cycle of 94°C for 3 min, followed by 35–40 cycles of 94°C for 15 s, 60–68°C for 15 s, and 72°C for 30 s. The primer sets used are listed in Table 1. PCR products were separated by electrophoresis on 1.5% agarose gels and were visualized with ethidium bromide staining.

RESULTS

Graft survival. All the isografts and allografts in mice administered monoclonal antibody against CD80 and CD86 from on *days 0* to *4* survived more than 100 days ($n = 5$, respectively). Mean graft survival time for

Table 1. *Primer pairs used in quantitative RT-PCR*

Gene	Accession No.	Sense (5′ → 3′)	Antisense (3′ → 5′)
HPRT	K01515	TGAAGAGCTACTGTAATGATCAGTCAAC	AGCAAGCTTGCAACCTTAACCA
MIG	M34815	ATTTCATCACGCCCTTGAGCCT	AAACAGACAGGCCTGGGATTTG
RANTES	AF065947	GCTGCCCTCACCATCATCCTCA	TTCTCTGGGTTGGCACACACTT
H2-Ea	V00833	GAATGTCNTGTGTGCTCTTGGGT	TGAAGNCATTGCCTCCAGGTAT
FRZB	U68058	CAAGCAGAGTAGCCCAACACCA	TGATTCCAGTGTGCCCCTTA
Gbp1	M55544	AATGTGGGAAGGCTCTGTGGTT	GAAAGGAAACACAGTAGGCT
Itgb2	M31039	AGCAGAAGGACGGAAGGAACAT	ACCAATCAGTACGACACCTA
Plaur	X62700	CTATGGGGCGTCCTCCTCTG	GGGCACACACATCCTCAAAG
TGFb	L19932	AAGGGGTTAAGGGGAGAAAGGT	TGTGAGCTCCAAGATGCCGTAG
IL1b	M15131	ACATCAGCACCTCACAAGCAGA	AGAAACAGTCCAGCCCATAC
Fn1	M18194	TTGAGCAGGAAAGTCACCCAGA	TTGAACACACANCCACAGGCCA
KRAB	AB024005	TACTTCTCAACATCAGACGA	GTTTTCCAATCACAGGGTCC
NFATc1	AF087434	TTCGTAAAGAGCACCGTGTC	ATACTGCATCACCAAGGGAG
Vav1	X64361	AAGTCGGCTGGTTTCCCTGTAA	AATGCTGATGGCGAACTCCG
Casp4	Y13089	TCCTGGCAACTGAGAACAAAGC	GTTGCTTAGGCTGGTCTTGA
Dcn	X53929	GATGTGTCTATGTGCGTTCTGC	GGGGTGTTTTTCCAGATTAT
Cox6a2	U08439	ACCACACGCTTTTCCACAATCC	ACTTCCACACCTTTATTGAG

cardiac allografts without administration of mAb (n = 5) was 8 ± 0.7 days (mean ± SD).

Histological findings. On *day 7*, tolerizing allografts exhibited a slightly diffuse, perivascular, or interstitial infiltration of mononuclear cells. Diffuse, perivascular, or interstitial infiltration of mononuclear cells and some foci of inflammatory infiltration with myocyte damage were observed in rejecting allografts. In addition, none of the isografts underwent rejection, as would be expected for inbred mouse strains (Fig. 2).

Reproducibility of the data. To verify the reproducibility of the data, the correlation among triplicate samples excised on *day 7* was investigated. We confirmed a strong linear correlation ($r > 0.95$; r is Pearson's correlation coefficient) between the gene expression profiles in the replicate samples of the same group (Fig. 3, *A–C*). On the other hand, there are larger alterations ($0.7 < r < 0.9$) in expression pattern between the genes of the isografts, rejecting allografts, and tolerizing allografts (Fig. 3, *D–F*).

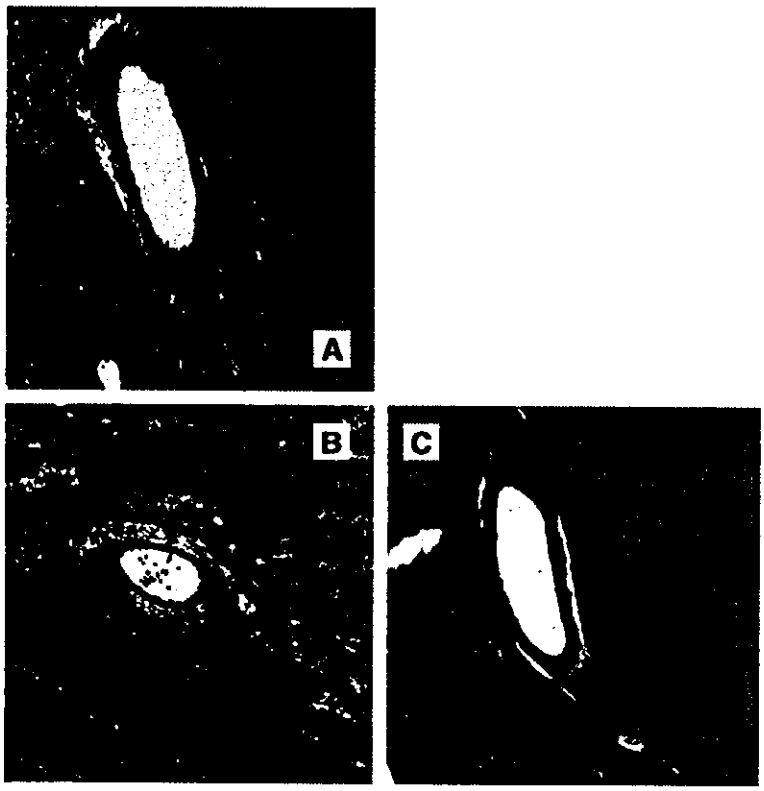

Fig. 2. Histology of transplanted hearts (*A–C*). On *day 7*, transplanted cardiac grafts were harvested and processed for hematoxylin and eosin staining. *A*: tolerizing allograft treated with mAbs 1G10 and GL1 from *days 0* to *4* daily. *B*: rejecting allograft. *C*: syngeneic isograft. Bar = 50 μm.

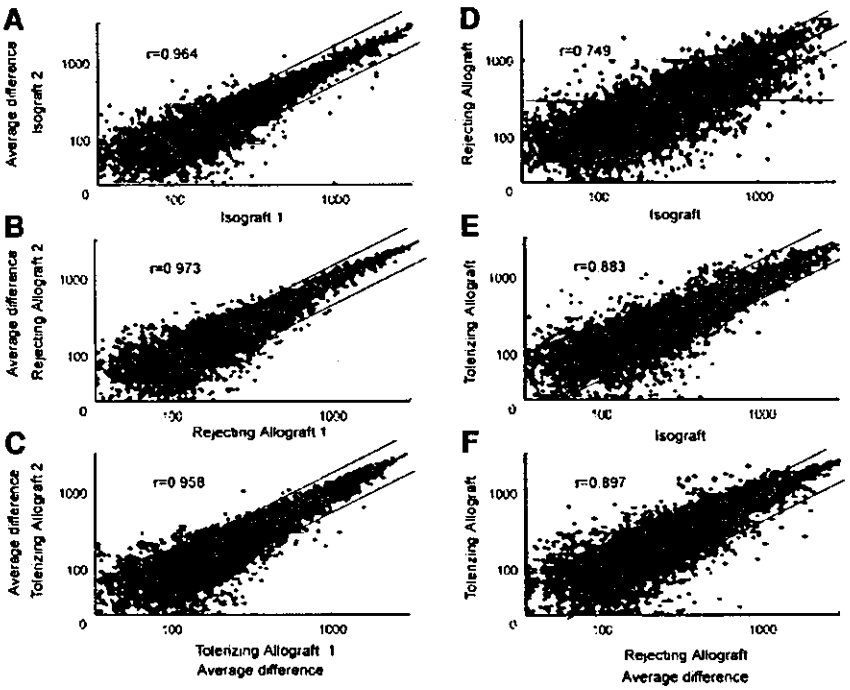

Fig. 3. Intra-experimental reproducibility of the data of hybridization on 12,488 probe sets on the MG-U74Av2 array (Affymetrix). Normalized signals of hybridization in the replicate samples are shown in the scatter graph of log (base 10) axes (*A–F*). The center line is $y = x$, and the flanking lines show the difference of a factor of 2. The proportion of genes that outlie these lines was less than 10% in all experiments. *r*, Pearson's linear correlation coefficient

Genes induced in tolerizing cardiac allografts. The analyses described in the METHODS revealed that 64 genes or expressed sequences tags (ESTs) were expressed to a significantly greater extent ($P \leq 0.05$) in the tolerizing allografts than in the syngeneic isografts on *day 7* (Fig. 1*A*; also, see Supplementary Table 1, available at the *Physiological Genomics* web site).[1] The same analyses performed in tolerizing vs. rejecting allografts elicited 16 genes to be induced more extensively in the tolerizing than rejecting allografts (Fig. 1*A*). The expression patterns of the former 64 genes were clustered by means of GeneSpring (Fig. 4*A*). Representative chemokine gene expression is shown in Fig. 4*B*. The average difference of not only the tolerizing but also the rejecting cardiac allografts on *day 7* was three times more than that of the syngeneic isografts on *day 7*. Fifty-six of these 64 genes were also induced more extensively in the rejecting allografts than syngeneic isografts. Genes identified commonly in both analyses of tolerizing allografts vs. syngeneic isografts and tolerizing vs. rejecting allografts were considered to be genes upregulated specifically in the tolerizing allografts (Fig. 1*A*). Two genes, histocompatibility 2, class II antigen Eα (H2-Ea) and secreted frizzled-related protein (FRZB) were identified, and the average difference and log ratio of these two genes are listed in Table 2. The expression pattern of H2-Ea is shown in Fig. 4*C*.

Genes induced in rejecting cardiac allografts. Next, we analyzed the gene expression induced in rejecting cardiac allografts. We had previously identified 84 genes or ESTs induced in rejecting cardiac allografts and had shown that IFN-γ-inducible genes are prominently induced in cardiac allografts (20). In this list of 84 genes, 66 probe sets were available in the setting of these experiments. Differential expression patterns of these 66 genes in isografts on *days 5*, *7*, and *70*, rejecting allografts on *days 5* and *7*, and tolerizing allografts on *days 5*, *7*, *28*, and *70* are shown in Fig. 5*A*. Interestingly, all of the preponderance of the genes profoundly induced in the rejecting allografts were also induced in the tolerizing cardiac allografts. We focused on chemotactic pro-inflammatory cytokine genes, especially on MIG and RANTES, because of the close relationship to the involvement in acute rejection (10, 20). The expression pattern of these two genes is shown in Fig. 4*B*. MIG and RANTES were also upregulated significantly ($P \leq 0.05$) in the tolerizing cardiac allografts. Furthermore, these gene expressions continued to be upregulated even on the 70th day after transplantation, more extensively in the tolerizing cardiac allografts than in the nonrejecting isografts.

Genes induced specifically in rejecting cardiac allografts. Many genes were upregulated both in the rejecting and tolerizing cardiac allografts. Therefore, we focused on the differential expression pattern between the two so as to identify a group of genes upregulated specifically in rejecting cardiac allografts. The criteria were the same as those performed to identify genes induced specifically in the tolerizing allografts, and the algorithm is shown in Fig. 1*B*. The analyses revealed that the expression of 21 genes was upregulated specifically in the rejecting allografts (Supplementary Ta-

[1]The Supplementary Material for this article (3 tables) is available online at **http://physiolgenomics.physiology.org/cgi/content/full/00086.2003/DC1**.

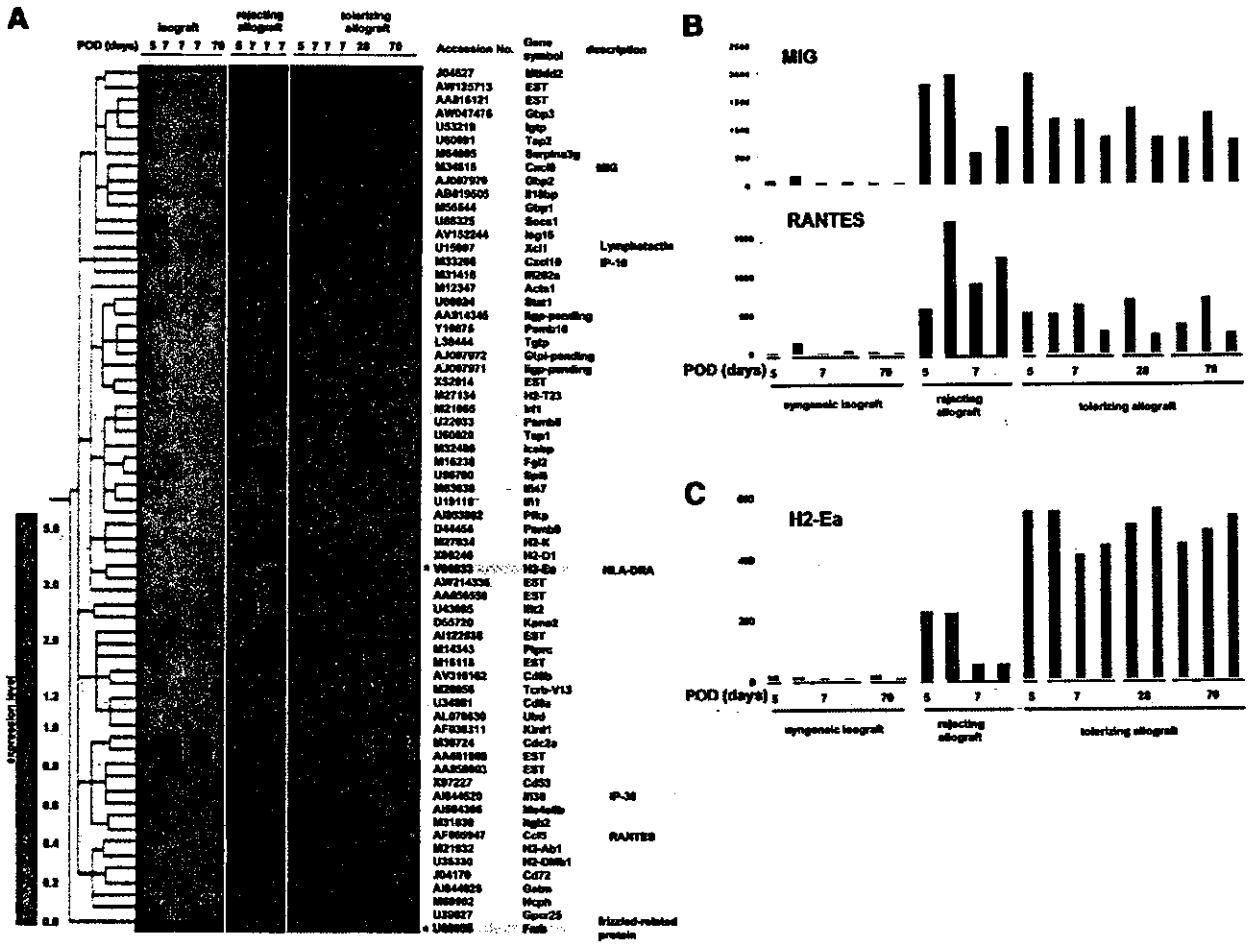

Fig. 4. *A*: the hierarchical clustering of 64 genes profoundly induced in tolerizing cardiac allografts on *day 7* compared with the syngeneic isografts on *day 7*. The average difference of the 64 genes upregulated more in the tolerizing allografts than in the syngeneic isografts were clustered by computer software (GeneSpring). Data are presented in a matrix format. Each row represents a single gene, and each column an experimental sample. The ratio of the abundance of transcripts of each gene to the median abundance of the gene's transcript is represented by a color in the corresponding sample in the matrix. Green squares, transcript levels below the median; red squares, transcripts levels above the median. Gene descriptions have been edited. Genes with asterisks were induced specifically in the tolerizing allografts on *day 7*. *B*: values of the average difference of representative chemokine genes, MIG and RANTES. The average difference of not only the tolerizing but also rejecting cardiac allografts on *day 7* was three times more than that of the syngeneic isografts on *day 7*. MIG, monokine induced by IFN-γ; RANTES, regulated on activation normal T cell expressed and secreted. *C*: values of the average difference in one of the genes upregulated specifically in the tolerizing allografts, H2-Ea.

ble 2). A clustering analysis of these 21 genes is shown in Fig. 5*B*.

Gene expressions in functional families. To characterize gene expression, we grouped the genes according to their functions (Fig. 6 and Supplementary Table 3). Hierarchical clustering revealed the expression of a large number of pro-inflammatory cytokines and chemokines was upregulated in both the rejecting and

Table 2. *Genes upregulated specifically in the tolerizing allograft on day 7*

Accession No.	Gene Symbol	Gene Description	*Day 7*			*Day 70*		*Day 7* Log Ratio		
			Syngeneic isograft	Rejecting allograft	Tolerizing allograft	Syngeneic isograft	Tolerizing allograft	Tol vs. Iso	Tol vs. Rej	Rej vs. Iso
V00833	H2-Ea	E-alpha gene for immune response gene	4.8 ± 2.9	105.3 ± 97.0	467.5 ± 75.1	9.0 ± 4.7	490.9 ± 45.9	6.78	2.52	4.46
U68058	Frzb	frizzled-related protein	29.8 ± 20.4	4.8 ± 1.3	101.9 ± 14.4	7.7 ± 0.1	14.2 ± 9.8	2.13	4.44	−2.64

Values are average differences ± SD and log ratios of the 2 genes, frizzled-related protein, and H2-Ea, induced specifically in the cardiac tolerizing allografts on *day 7*. Tol, tolerizing cardiac allografts; Iso, syngeneic cardiac isografts; Rej, rejecting cardiac allografts.

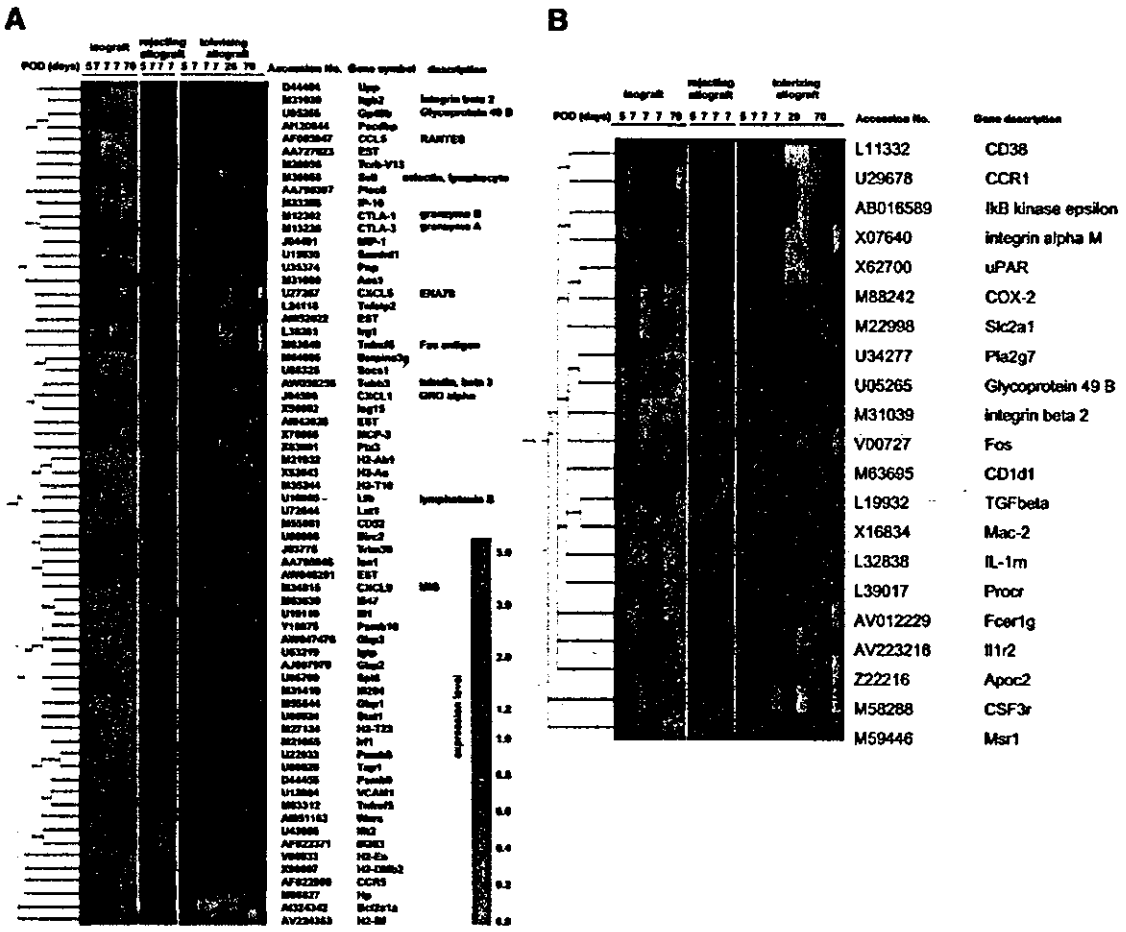

Fig. 5. *A*: hierarchical clustering of genes induced in rejecting cardiac allografts on *day 7*. We previously identified 84 genes profoundly induced in rejecting cardiac allografts (10). In this experiment, 66 of the 84 genes were available to be monitored. Gene expression patterns of a set of the 66 genes, which were induced in rejecting cardiac allografts on *day 7*, were clustered using a hierarchical clustering computer program (*GeneSpring*). *B*: hierarchical clustering of 21 genes upregulated specifically in rejecting cardiac allografts on *day 7* compared with syngeneic cardiac isografts and tolerizing cardiac allografts on *day 7*.

tolerizing allografts. MIG, RANTES, IP-10, and MCP-2 and their receptors CCR1, CCR5, and CXCR3 were induced not only in the rejecting but also in the tolerizing allografts on *day 7* (Fig. 6*A*).

In a group of adhesion molecule, signal transduction, and apoptosis-related genes, most of the expression patterns were found to be prominent not only in the rejecting but also in the tolerizing allografts. In contrast, we were able to identify a group of genes that was downregulated exclusively in the rejecting allografts in a group of genes related to cell structure/motility and cell metabolism (Fig. 6*B*).

Validation of gene expression data by quantitative RT-PCR. To further validate the microarray data on changes in gene expression, certain representative genes upregulated specifically in the tolerizing and rejecting allografts, as well as genes of their functional families, were analyzed by quantitative RT-PCR (Fig. 7). The microarray data expression patterns were verified for the 16 genes except Fn1, KRAB, FRZB, and Casp4. In particular, the expression patterns of three of the genes (Itgb2, Gbp1, and Dcn) were found to have a perfect match between their quantitative RT-PCR and DNA microarray data in terms of patterns of statistical significance.

Compared with the deteriorated expression in the isografts on *days 7* and *70*, the expression of MIG and RANTES continued to be upregulated in both groups of the rejecting and tolerizing allografts, which correlated well with the data from the DNA microarray.

DISCUSSION

We describe the gene expression profile of tolerizing cardiac allografts compared with syngeneic isografts and rejecting allografts. It proved possible to identify the prominent gene expression of many putative pro-inflammatory cytokines and chemokines in tolerogenic allografts. Our results indicate that these pro-inflammatory cytokines and chemokines are closely associ-

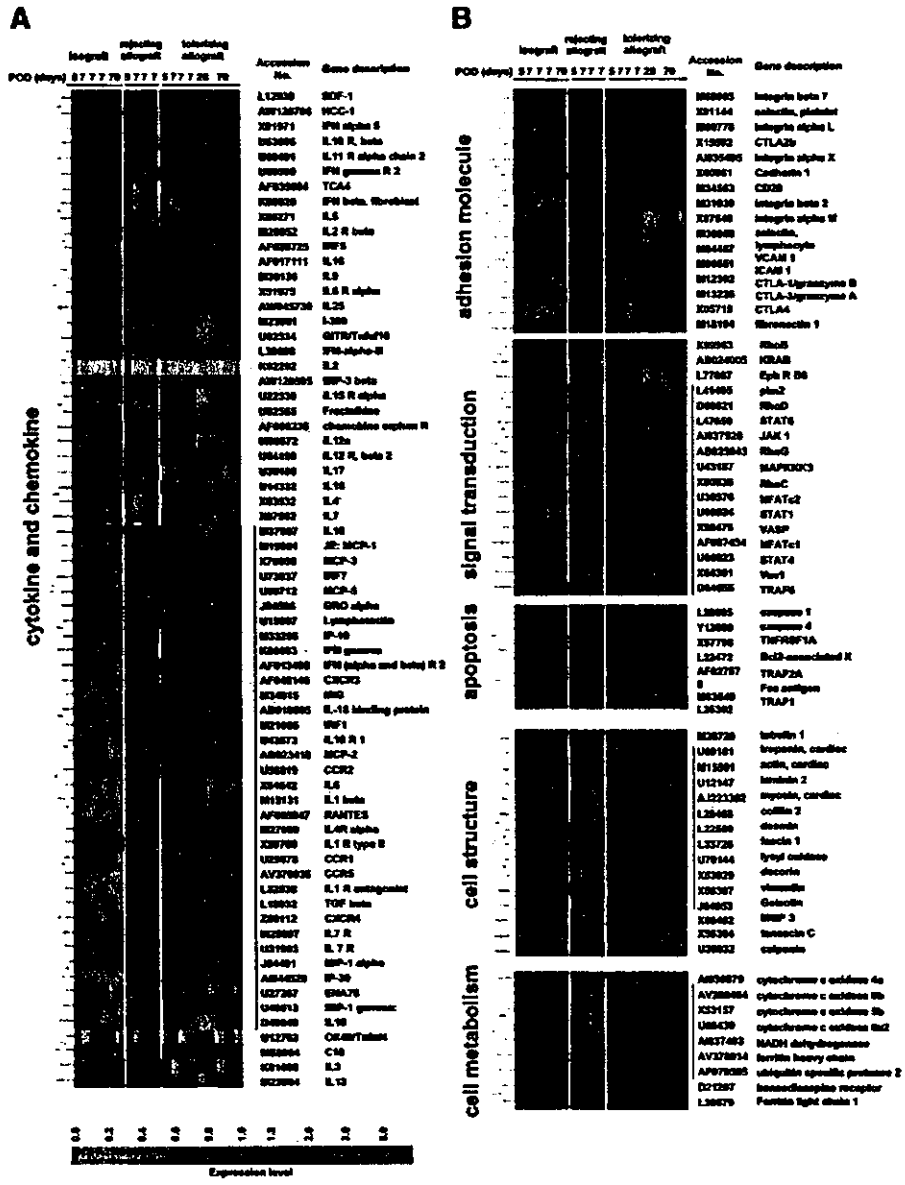

Fig. 6. Gene expressions in functional families. In each cluster, genes were clustered according to the similarity of their expression patterns.

ated with tolerance induction by costimulatory blockade.

In this study, we demonstrated the similarity of gene expression profile in the states of acute rejection and tolerance. No effective regimen has succeeded in inducing tolerance in clinical organ transplantation (19). Our findings point to an association between the induction of tolerance and many functional signals including inflammation, apoptosis, and signal transduction. It is interesting that marked expression of genes for various kinds of pro-inflammatory cytokines, chemokines, and adhesion molecules did not break the tolerance state. Moreover, these genes continued to be upregulated even 70 days after transplantation. These findings suggest that these genes have no deleterious effects on the tolerance state not only in the induction phase but also in the maintenance phase.

Recent reports support the idea that calcineurin-NFAT signaling is absolutely required in the induction of tolerance both in vitro and in vivo (17). Although the current immunosuppressive regimens have dramatically improved early survival after transplantation, they have failed to induce tolerance. Paradoxically, tolerance induction by costimulatory blockade is hindered by calcineurin inhibitors and steroids (12, 15), which are commonly employed in the standard regimen of immunosuppressant drugs after organ transplant. This may be one of the reasons for the failure to date of all attempts to induce tolerance after organ transplantation. Another studies have demonstrated a

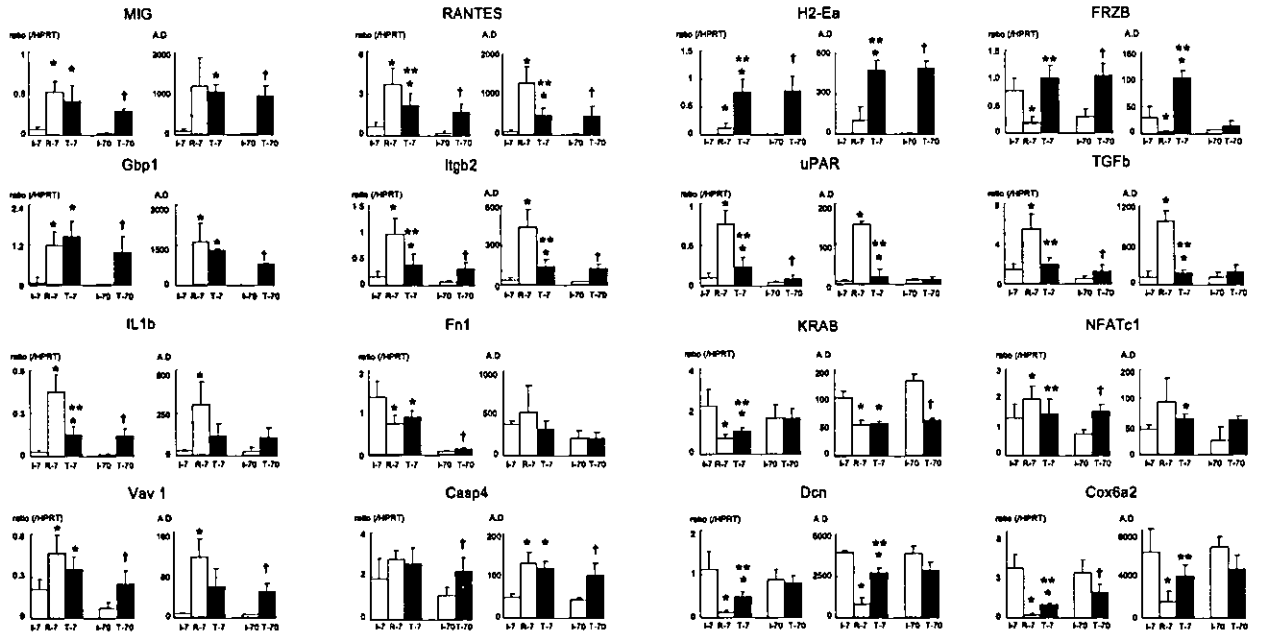

Fig. 7. Validation of the expression profile of the 16 genes by quantitative RT-PCR. Genes were singled out from the results of the comparative analyses shown in Figs. 4–6. Two graphs are illustrated for each gene. The one on the *left* depicts the results of the quantitative RT-PCR, and the one on the *right* depicts the results of the DNA microarray. Mean values are presented within each column, and the bars indicate the standard deviation from the mean. AD, average difference; I-7, syngeneic isografts on *day 7*; R-7, rejecting allografts on *day 7*; T-7, tolerizing allografts on *day 7*; I-70, syngeneic isografts on *day 7*; T-70, tolerizing allografts on *day 7*. *Statistically significant ($P \leq 0.05$) compared with syngeneic isografts on *day 7*. **Statistically significant ($P \leq 0.05$) compared with rejecting allografts on *day 7*. †Statistically significant ($P \leq 0.05$) compared with syngeneic isografts on *day 7*.

requirement for activation-induced cell death of T cells in tolerance induction (13). IL-2 and IFN-γ promote activation-induced cell death (1, 3, 7). These are consistent with our results demonstrating prominent expressions of apoptosis-related genes. Our data revealed prominent IFN-γ signaling both in rejecting and tolerizing cardiac allografts. Taken together, it may be that IFN-γ signaling contributes to tolerance induction by promoting the activation-induced cell death of T cells. If so, costimulatory blockade together with immunosuppressive drugs which do not block the signaling of IFN-γ or IL-2, such as mycophenolate mofetil, sirolimus, or IL-2 receptor antibodies, would be more feasible in the induction of tolerance after clinical transplantation.

In contrast to isografts, moderate mononuclear cell infiltrations were observed in the tolerizing cardiac allografts on *day 7*. Recruitment of mononuclear cells into the graft appears to be an essential step for tolerance induction. Pro-inflammatory cytokines or chemokines may play a pivotal role in this step by helping to recruit these mononuclear cells. It is interesting that despite mononuclear cell infiltrations indefinite graft survival can be achieved in the tolerizing allografts. A group of genes related to cell structure and motility were exclusively suppressed in the rejecting allografts. Consistent with the macroscopic viability and indefinite graft survival, these data indicate the viability of the graft. Some as yet unknown mechanism which inactivates the infiltrated cells ability to attack the graft protects the tolerizing graft from rejection.

Recently, AP-1 signaling was selectively suppressed in tolerizing allografts compared with rejecting allografts (17). We analyzed 14 of the 17 genes reported in that study. The 14 genes were not altered in either the tolerizing or rejecting allografts in our study. Further study will be necessary to identify how the difference in gene expression between the rejecting and tolerizing allografts actually determines the different outcomes, as well as to clarify the molecular mechanism of immunologic tolerance.

Although DNA microarray analysis had previously shown the similarity of gene expression in cardiac rejecting and tolerizing allografts, we were able to identify only a few genes, e.g., H2-Ea and secreted frizzled-related protein (FRZB), as specifically induced in the tolerizing cardiac allografts. H2-Ea in the mouse is a homologous gene of human lymphocyte antigen (HLA) DR-α in humans, and in clinical renal transplantation HLA-DR matching of cadaveric kidneys has been shown to improve survival of the graft (18). FRZB is an antagonist of Wnt signaling, which has an important role in the differentiation and patterning of tissues in animal development (8). We could not identify the mechanism by which the induced gene expressions of H2-Ea and FRZB in the tolerizing cardiac allografts contribute to the induction and maintenance of tolerance. It is expected that future work will elucidate both, and ultimately afford us an insight into how tolerance can be manipulated in the clinical setting.

DNA microarray technology is a powerful tool in an unbiased assessment of expression levels of thousands of genes simultaneously, but there are several issues which must be kept in mind when interpreting the results this technology yields (9, 16). First, most studies are performed with a rather more limited number of repetitions than might be optimally desirable, because of the high cost of microarray studies, and reducing the number of replications could conceivably lead to false-positive results. Another point to keep in mind is that the validity of the data often depends on the experimental settings and the investigator's technical skills. Our previous investigations led to reports of a good correlation of the data obtained by DNA microarray and Northern blotting. We demonstrated a reliable reproducibility of the data between replicate experiments. Second, the correlation between the mRNA and the target protein relative abundance in the cell may not be straightforward. This issue is undoubtedly problematic, but the actual absence of mRNA in the cell is certainly likely to imply a not very high level of the respective protein (5). Therefore, our current data with a set of replicate samples can provide us adequate information. Finally, it is difficult to detect a weak gene expression signal by means of DNA microarray technology. Such diminished but yet still biologically important gene expression could well be masked by other vigorous gene expressions.

In this study, we have reported the gene expression profile of tolerizing allografts in a murine cardiac transplant model. Our findings indicate that immunological tolerance can be induced and maintained even in the face of marked pro-inflammatory gene expression in vivo. The DNA microarray has provided us with new insight into the molecular mechanisms of immunological tolerance after costimulatory blockade.

ACKNOWLEDGMENTS

We thank Y. Hippo, T. Shimamura, S. Yamamoto, and N. Nishikawa for valuable comments and H. Kato, T. Hasegawa, M. Kinoshita, and M. Washida for excellent technical assistance, and K. Boru of Advanced Clinical Trials, Inc., for review of the manuscript.

GRANTS

This study was supported in part by a grant from R&D projects in Cooperation with Academic Institutions, Aid for Advanced Forefront Medical Development, 2000–2002, the Yamanouchi Foundation for Research on Metabolic Disorders, the Mitsubishi Pharma Research Foundation, and the Takeda Science Foundation.

REFERENCES

1. **Badovinac VP, Tvinnereim AR, and Harty JT.** Regulation of antigen-specific CD8+ T cell homeostasis by perforin and interferon-gamma. *Science* 290: 1354–1358, 2000.
2. **Bashuda H, Seino K, Kano M, Sato K, Azuma M, Yagita H, and Okumura K.** Specific acceptance of cardiac allografts after treatment with antibodies to CD80 and CD86 in mice. *Transplant Proc* 28: 1039–1041, 1996.
3. **Bishop DK, Chan Wood S, Eichwald EJ, and Orosz CG.** Immunobiology of allograft rejection in the absence of IFN-gamma: CD8+ effector cells develop independently of CD4+ cells and CD40-CD40 ligand interactions. *J Immunol* 166: 3248–3255, 2001.
4. **Brown PO and Botstein D.** Exploring the new world of the genome with DNA microarrays. *Nat Genet* 21: 33–37, 1999.
5. **Celis JE, Kruhoffer M, Gromova I, Frederiksen C, Ostergaard M, Thykjaer T, Gromov P, Yu J, Palsdottir H, Magnusson N, and Orntoft TF.** Gene expression profiling: monitoring transcription and translation products using DNA microarrays and proteomics. *FEBS Lett* 480: 2–16, 2000.
6. **Corry RJ, Winn HJ, and Russell PS.** Primarily vascularized allografts of hearts in mice. The role of H-2D, H-2K, and non-H-2 antigens in rejection. *Transplantation* 16: 343–350, 1973.
7. **Dalton DK, Haynes L, Chu CQ, Swain SL, and Wittmer S.** Interferon gamma eliminates responding CD4 T cells during mycobacterial infection by inducing apoptosis of activated CD4 T cells. *J Exp Med* 192: 117–122, 2000.
8. **Dann CE, Hsieh JC, Rattner A, Sharma D, Nathans J, and Leahy DJ.** Insights into Wnt binding and signalling from the structures of two Frizzled cysteine-rich domains. *Nature* 412: 86–90, 2001.
9. **Eisen MB and Brown PO.** DNA arrays for analysis of gene expression. *Methods Enzymol* 303: 179–205, 1999.
10. **Fahmy NM, Yamani MH, Starling RC, Ratliff NB, Young JB, McCarthy PM, Feng J, Novick AC, and Fairchild RL.** Chemokine and chemokine receptor gene expression indicates acute rejection of human cardiac transplants. *Transplantation* 75: 72–78, 2003.
11. **Isobe M, Yagita H, Okumura K, and Ihara A.** Specific acceptance of cardiac allograft after treatment with antibodies to ICAM-1 and LFA-1. *Science* 255: 1125–1127, 1992.
12. **Kirk AD, Burkly LC, Batty DS, Baumgartner RE, Berning JD, Buchanan K, Fechner JH Jr, Germond RL, Kampen RL, Patterson NB, Swanson SJ, Tadaki DK, TenHoor CN, White L, Knechtle SJ, and Harlan DM.** Treatment with humanized monoclonal antibody against CD154 prevents acute renal allograft rejection in nonhuman primates. *Nat Med* 5: 686–693, 1999.
13. **Lenardo MJ.** Interleukin-2 programs mouse alpha beta T lymphocytes for apoptosis. *Nature* 353: 858–861, 1991.
14. **Li XC, Strom TB, Turka LA, and Wells AD.** T cell death and transplantation tolerance. *Immunity* 14: 407–416, 2001.
15. **Li Y, Zheng XX, Li XC, Zand MS, and Strom TB.** Combined costimulation blockade plus rapamycin but not cyclosporine produces permanent engraftment. *Transplantation* 66: 1387–1388, 1998.
16. **Lipshutz RJ, Fodor SP, Gingeras TR, and Lockhart DJ.** High density synthetic oligonucleotide arrays. *Nat Genet* 21: 20–24, 1999.
17. **Macian F, Garcia-Cozar F, Im SH, Horton HF, Byrne MC, and Rao A.** Transcriptional mechanisms underlying lymphocyte tolerance. *Cell* 109: 719–731, 2002.
18. **Moen T, Albrechtsen D, Flatmark A, Jakobsen A, Jervell J, Halvorsen S, Solheim BG, and Thorsby E.** Importance of HLA-DR matching in cadaveric renal transplantation: a prospective one-center study of 170 transplants. *N Engl J Med* 303: 850–854, 1980.
19. **Monaco AP.** Strategies for induction of clinical tolerance. *Transplant Proc* 33: 51–56, 2001.
20. **Saiura A, Mataki C, Murakami T, Umetani M, Wada Y, Kohro T, Aburatani H, Harihara Y, Hamakubo T, Yamaguchi T, Hasegawa G, Naito M, Makuuchi M, and Kodama T.** A comparison of gene expression in murine cardiac allografts and isografts by means DNA microarray analysis. *Transplantation* 72: 320–329, 2001.
21. **VanBuskirk AM, Pidwell DJ, Adams PW, and Orosz CG.** Transplantation immunology. *JAMA* 278: 1993–1999, 1997.
22. **Wells AD, Li XC, Li Y, Walsh MC, Zheng XX, Wu Z, Nunez G, Tang A, Sayegh M, Hancock WW, Strom TB, and Turka LA.** Requirement for T-cell apoptosis in the induction of peripheral transplantation tolerance. *Nat Med* 5: 1303–1307, 1999.
23. **Yang J, Moravec CS, Sussman MA, DiPaola NR, Fu D, Hawthorn L, Mitchell CA, Young JB, Francis GS, McCarthy PM, and Bond M.** Decreased SLIM1 expression and increased gelsolin expression in failing human hearts measured by high-density oligonucleotide arrays. *Circulation* 102: 3046–3052, 2000.

Jpn J Clin Oncol 2003;33(12)613–619

Intratumor Microvessel Density in Biopsy Specimens Predicts Local Response of Hypopharyngeal Cancer to Radiotherapy

Shi-Chuan Zhang[1,3], Shin-ichi Miyamoto[1], Tomoyuki Kamijo[2], Ryuichi Hayashi[2], Takahiro Hasebe[1], Genichiro Ishii[1], Masashi Fukayama[3] and Atsushi Ochiai[1,4]

[1]Pathology Division, National Cancer Center Research Institute East, Kashiwa, Chiba, [2]Department of Head and Neck Surgery, National Cancer Center Hospital East, Kashiwa, Chiba, [3]Pathology Division, Graduate School of Medicine, University of Tokyo, Tokyo and [4]Laboratory of Cancer Biology, Graduate School of Frontier Science, University of Tokyo, Kashiwa, Chiba, Japan

Received August 26, 2003; accepted November 18, 2003

Background: The aim of this retrospective study was to identify reliable predictive factors for local control of hypopharyngeal cancer (HPC) treated by radiotherapy.
Methods: A cohort of 38 patients with HPC treated by radical radiotherapy at the National Cancer Center Hospital East between 1992 and 1999 were selected as subjects for the present study. Paraffin-embedded pre-therapy biopsy specimens from these patients were used for immunostaining to evaluate the relationships between local tumor control and expression of the following previously reported predictive factors for local recurrence of head and neck cancer treated by radiotherapy: Ki-67, Cyclin D1, CDC25B, VEGF, p53, Bax and Bcl-2. The predictive power of microvessel density (MVD) in biopsy specimens and of clinicopathologic factors (age, gender and clinical tumor-node-metastasis stage) was also statistically analyzed.
Results: Twenty-five patients developed tumor recurrence at the primary site. Univariate analysis indicated better local control of tumors with high microvessel density [MVD ≥ median (39 vessels/field)] than with low MVD (< median, $P = 0.042$). There were no significant associations between local control and expression of Ki-67 ($P = 0.467$), Bcl-2 ($P = 0.127$), Bax ($P = 0.242$), p53 ($P = 0.262$), Cyclin D1 ($P = 0.245$), CDC25B ($P = 0.511$) or VEGF ($P = 0.496$). Clinicopathologic factors were also demonstrated to have no significant influence on local control (age, $P = 0.974$; gender, $P = 0.372$; T factor, $P = 0.602$; N factor, $P = 0.530$; Stage, $P = 0.499$).
Conclusion: Microvessel density in biopsy specimens was closely correlated with local control of HPC treated by radiotherapy.

Key words: hypopharyngeal cancer – radiosensitivity – predictive factor – microvessel density

INTRODUCTION

Radical radiotherapy or chemoradiotherapy of hypopharyngeal cancer (HPC) has the potential advantage over surgery of less cosmetic and functional loss. However, if it fails, the alternative curative surgery will be delayed and the complications of treatment will increase. Although it is important for clinicians to determine if an individual with HPC should be treated by radiotherapy or chemoradiotherapy as initial therapy or the main modality, there is no generally applicable indicator of the radiocurability of HPC available as yet.

One potential biological marker for radiocurability is surviving fraction at 2 Gy (SF2), which reflects intrinsic tumor radiosensitivity, but studies in this area have not led to any consensus that this can be clinically used as a predictor of tumor recurrence (1,2). As a result of a recent increase in our knowledge of tumor molecular biology, interest is now being focused on molecules involved in cell signal transduction, cell-cycle control, tumor angiogenesis and apoptosis pathways, and there is a long list of candidate molecules that includes p53, Bax, Bcl-2, EGFR, VEGF, Cyclin D1 and CDC25B (3–8).

Tumor hypoxia accounts for the major portion of the radioresistance mechanism in tumors treated by irradiation with low energy transfer (LET), including X-rays and γ-rays, and indicators of tumor hypoxia should predict the radioresponse. However, only a few papers have assessed the hypoxia indicators, hypoxia induced factor-α (HIF-α) or tumor PO_2, as prognostic factors after radiotherapy (9–11).

For reprints and all correspondence: Atsushi Ochiai, Pathology Division, National Cancer Center Research Institute East, Laboratory of Cancer Biology, Graduate School of Frontier Science, University of Tokyo, 6-5-1, Kashiwanoha, Kashiwa, Chiba 277-8577, Japan.
E-mail: aochiai@east.ncc.go.jp

Since tumor radiosensitivity is thought to be influenced by multiple factors involved in several cell survival pathways, we investigated the predictive power of the following factors for local control rate of HPC treated by radiotherapy or chemoradiotherapy: Ki-67 as a proliferative factor; Cyclin D1 and CDC25B as cell cycle modifiers; p53, Bcl-2 and Bax as apoptosis factors; and vascular endothelial growth factor (VEGF) as an angiogenesis factor, all of which were previously reported to be predictive for radiosensitivity of head and neck cancer. In addition to these markers, we also investigated whether tumor microvessel density (MVD) can be used as a potential hypoxia marker to predict tumor local recurrence in HPC. We also assessed the clinicopathologic factors of patients which might affect local tumor control by radiotherapy.

PATIENTS AND METHODS

PATIENTS

A cohort of 38 patients with HPC treated by radical radiotherapy or chemoradiotherapy at the National Cancer Center Hospital East between 1992 and 1999 were selected as subjects for this study. Required inclusion criteria included: (i) previously untreated, (ii) local control followed up for more than 6 months, (iii) no death from intermittent disease, (iv) biopsy specimen adequate for immunohistological analysis and (v) no further treatment at the primary site during the follow-up period. The characteristics of all 38 cases are listed in Table 1. A total of 43 specimens were used for analysis (two specimens each were taken from five cases).

All 38 patients received curative dose of 60–72 Gy at the primary site. TNM classification was performed according to the criteria of the Union International Contre le Cancer (UICC). All biopsy specimens were taken from the primary sites before treatment and diagnosed as squamous cell carcinoma. Twenty-five patients developed recurrence at the primary site. The mean local disease-free interval was 14.9 months (range, 1–94.2 months).

Table 1. Clinicopathologic features of 38 HPC patients

Variable	Number of patients
Total number of patients	38
Clinical features	
Gender	
Male	35
Female	3
Age (years)	
Mean	62.8
Range	41–83
Pathological features	
Tumor location	
Posterior wall	6
Post cricoid	1
Pyriform sinus	31
T factor	
1	4
2	17
3	13
4	4
N factor	
0	11
1	7
2	10
3	10
Histological differentiation	
Well diff, SCC	4
Moderated diff, SCC	27
Poor diff, SCC	7

TREATMENT

Of the 38 patients, 17 were treated by conventional fractionated radiotherapy and 21 were given two courses of 30 Gy radiation with concurrent administration of cisplatin (bolus injection of 40 mg/m^2 on days 1 and 8) and 5-FU (continuous infusion of 200 mg/m^2 on days 1–4 and 8–11) with 2 weeks rest. The dose in the second course could be raised to a maximum of 42 Gy according to the tumor response.

IMMUNOHISTOCHEMICAL STAINING

The immunohistochemical staining method has been described elsewhere (12). Formalin-fixed, paraffin-embedded specimens were cut into 4 μm-thick sections, then deparaffinized in xylene and dehydrated through graded alcohol. Endogenous peroxidase activity was inhibited by immersion in 0.3% H_2O_2 for 20 min. For antigen retrieval, the sections were heated in a microwave oven (750 W, 20 min in citrate buffer) or autoclaved at 121°C for 10 min (for anti-Bax). Non-specific conjugation was blocked with 2% normal bovine serum. The slides were incubated overnight at 4°C with the following different antibodies: (i) an anti-Ki-67 antibody (MIB-1; 1:50 dilution; DAKO, Glostrup, Denmark), (ii) an anti-Bax antibody (1:50 dilution; Calbiochem, Cambridge, MA), (iii) an anti-Bcl-2 antibody (1:40 dilution; DAKO), (iv) an anti-Cyclin D1 antibody (1:400 dilution; Santa Cruz, Santa Cruz, CA), (v) an anti-CDC25B antibody (1:100 dilution; Santa Cruz), (vi) an anti-VEGF antibody (1:100 dilution; Santa Cruz), (vii) an anti-p53 antibody (1:20 000 dilution; Nichirei, Chiba, Japan) and (viii) an anti-CD31 antibody (1:50 dilution; DAKO). After washing in PBS, tissues were incubated with biotin-labeled anti-rabbit or anti-mouse second antibodies (Vector Laboratories Inc., Burlingame, CA) for 30 min at room temperature and then reacted with streptavidin–biotin horseradish peroxidase complex (DAKO) for 30 min. The reaction products were

visualized by immersing the slides in freshly prepared diaminobenzidine solution for 5–20 min and counterstained with hematoxylin before dehydration and mounting.

Evaluation for Immunostaining

All immunostained tissue sections were evaluated in a coded manner without knowledge of the clinical and pathological parameters. To evaluate Ki-67, p53 and Cyclin D1, the number of brown-stained tumor nuclei per total number of tumor cells in the most highly stained area on each slide was counted in the selected microscopic field at ×200. A total of 571–1000 tumor cells were examined in each specimen. As in previous studies (12), when >40% of tumor cells were stained positive Ki-67, the tumor was evaluated as positive. For p53 and Cyclin D1, the tumor was considered positive when 10% and 30%, respectively, of the cells were stained positive. Bcl-2 and CDC25B staining was localized to the cell cytoplasm, and sections in which >10% of the tumor cells stained positive were categorized as positive. VEGF and Bax immunostaining was semiquantitatively rated on a 4-grade scale (0, +, ++, +++) according to the intensity of the reaction and extent of staining and patients were divided into two groups (0, + versus ++, +++) for statistical analysis. CD31-stained sections were scanned at low magnification (×40) to determine areas with the highest number of microvessels (hot spots). Microvessels were counted at a magnification of ×200 in two hot spots on each section and MVD was calculated as the average of the two measurements. For the five cases with two specimens, hot spots were counted in each specimen and the average of the highest two was recorded as MVD.

Statistical Analysis

Univariate analysis for tumor-free survival was performed using log-rank tests. The survival curves were calculated by the Kaplan–Meier method. $P < 0.05$ was considered significant. Statistical analysis was performed with the Statistica package (Statsoft, Tulsa, OK).

RESULTS

Clinicopathologic Factors and Local Control of HPC Treated by Radiotherapy Alone or by Chemoradiotherapy

The cohort was composed of 35 men (92%) and three women (8%) with a mean age at the time of diagnosis of 62.8 years (range 41–83, Table 1). In 31 cases the tumor was located in pyriform, in six cases in posterior wall (15.8%) and in one case in post cricoid (2.6%). Twenty-one patients had an early T classification (T1 and T2: 55.3%). Approximately two thirds of the patients had a positive N classification (N1–N3: 71.1%), and the majority of cases were in an advanced clinical stage (stage III stage IV: 81.6%). Univariate analysis showed no significant associations between local control and any of the clinicopathologic parameters (Table 2) and no relation between local control and concurrent administration of low dose of 5-FU and cisplatin with radiotherapy (Table 2).

Table 2. Local tumor-free survival analysis of clinicopathologic factors for 38 patients with HPC treated with radiotherapy/chemoradiotherapy

Variable	*n*	*P* value
Age		
<62.8	18	
≥62.8	20	0.974
Gender		
Female	3	
Male	35	0.372
T factor		
T1–2	21	
T3–4	17	0.602
N factor		
N0	11	
N1–3	27	0.530
Stage		
I, II	7	
III, IV	31	0.499
Chemo*		
–	17	
+	21	0.589

*Chemo, radiotherapy concurrent with chemotherapy.

Immunohistological Factors and Local Control by Radiotherapy or Chemoradiotherapy

Positive staining for Ki-67, p53 (Fig. 1A), Cyclin D1 (Fig. 1B), CDC25B, Bax, Bcl-2 (Fig. 1C) and VEGF was observed in 26, 16, 21, 24, 20, 10 and 16, respectively, of the 38 cases (68%, 42%, 55%, 61%, 53%, 26% and 42%, respectively). In the univariate analysis, none of these factors was significantly related to local control by radiotherapy/chemoradiotherapy (Table 3).

MVD and Local Control by Radiotherapy or Chemoradiotherapy

After immunostaining with anti-CD31 antibody, brown-stained lumens in the tumor tissue were counted as blood vessels (Fig. 1D). MVD ranged from 5 to 74 microvessels per field (= 0.391 mm^2). Since the median MVD was 39 microvessels/field, the tumors were divided into a high MVD group (MVD ≥ median) and a low MVD group (MVD < median). Univariate analysis showed a significant relation between higher MVD and better local control by radiotherapy ($P = 0.042$).

Considering that five cases were analyzed with two specimens each there may be bias of MVD count between the two specimens. We randomly divided these specimens into two groups and performed the univariate analysis for local tumor-

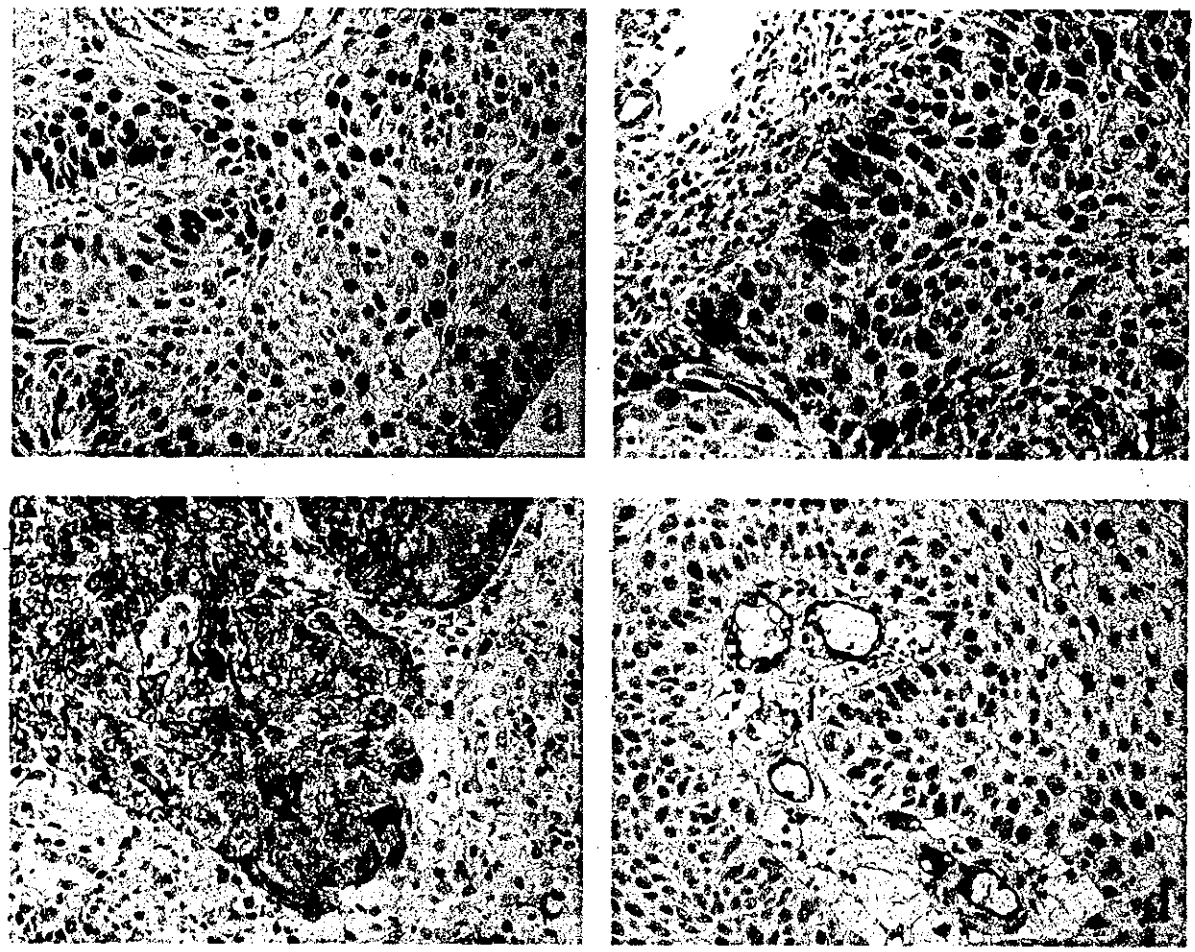

Figure 1. Representative photomicrographs of immunostaining results. (A) An example of p53 staining. Tumor cell nuclei are stained brown. (B) Nuclear staining of Cyclin D1. (C) An example of positive Bcl-2 staining, with 100% tumor-cell cytoplasm stained. (D) An example of CD31 staining. Tumor blood vessels were countable after staining.

free survival of 38 cases, respectively. The results from these two groups were the same as we had initially found (P = 0.042). In fact, both groups had the same median MVD count as the first, which will not influence the result of primary statistical analysis (Table 4).

Survival Curves According to MVD by Kaplan–Meier Analysis

Since univariate analysis showed that only MVD was correlated with local control, we performed the Kaplan–Meier analysis to assess the predictive value of MVD for local control of HPC treated by radical radiotherapy or by chemoradiotherapy. The results are shown in Figure 2. The local control rate 3 years after treatment was 58% among those with high MVD, as opposed to only 21% among those with low MVD ($P = 0.042$).

DISCUSSION

Few studies have specifically assessed the radiosensitivity of HPC. Our knowledge about predictive factors for the radioresponse of HPC basically comes from previous studies on various sites of head and neck cancers. In the current study, we assessed the predictive value of factors that have been reported to be related to the radiosensitivity of head and neck cancer in the area of HPC. An important result of this study was that local control of HPC after radiotherapy or chemoradiotherapy is strongly associated with the intratumor MVD of biopsy specimens, suggesting that the MVD of biopsy specimens may be of help in predicting the radioresistance of HPC.

It is well known that tumor hypoxia causes radioresistance of solid tumors, and indicators of tumor hypoxia have long been thought of as predictive factors of tumor radioresistance. Measurement of PO_2 obtained with polargraphic electrode has been reported to be a predictor of the therapeutic response of head and neck cancers to radiotherapy (10,11). However, its invasive nature restricts measurements to easily accessible tumors and may impede their clinical application. HIF1-α is a key transcription factor induced by hypoxia and regulates the pathways of angiogenesis, glycolysis, growth-factor signaling and other essential adaptive responses to hypoxia. Aebersold et al. reported expression of HIF-1α in oropharyngeal cancer to be an independent predictive factor of tumor radioresponse (9). In addition, a study on cervical cancer xenografts suggested

Table 3. Local tumor-free survival analysis of molecular factors for 38 patients with HPC treated with radiotherapy/chemoradiotherapy

Variable	*n*	*P* value
Ki-67		
<40%	12	
≥40%	26	0.467
Bcl-2		
<10%	28	
≥10%	10	0.127
Bax		
0, +	18	
+, ++	20	0.242
p53		
<10%	22	
≥10%	16	0.262
Cyclin D1		
<30%	17	
≥30%	21	0.245
CDC25B		
<10%	14	
≥10%	24	0.511
VEGF		
0, +	22	
+, ++	16	0.496
MVD		
<39	19	
≥39	19	0.042

that the spatial distribution of HIF-1α colocalized with the nitroimidazole hypoxia marker EF5 and warranted further study of the relationship between HIF-1α and radiosensitivity (13). Tumor cells obtain oxygen and nutrients from neighboring blood flows. As early as 1955, Thomlinson and Gray found that oxygen diffusion from blood vessels to tumor tissues has a distance limitation of about 150 μm (14), which suggested tumor oxygen profile is determined by its vasculature. In fact, we have shown that intratumor MVD is correlated with local control rate in laryngeal cancer treated by radiotherapy (12). In the present study, we also showed that MVD is a predictor for the local control of radiation-treated HPCs.

Although many studies, including the present one, have shown that higher MVD in tumor biopsy specimen significantly correlates with better radioresponse, some investigators have argued that, since angiogenesis is induced by hypoxia, neovasculature should be taken as an indicator of hypoxia (15). In the present study, newly-formed vessels, which appeared as single endothelial cells in the section, were excluded from the vessel count. An area with active angiogenesis may not have a high vessel count in this study. Although the tumor vascular network of solid tumors holds more non-functional vessels

Table 4. Different MVD count between two specimens from one tumor

Patient	Group 1	Group 2
1	9/9 (9)	13/11 (12)
2	50/48 (49)	40/43 (41.5)
3	6/7 (6.5)	7/8 (7.5)
4	25/23 (24)	18/12 (15)
5	29/24 (26.5)	35/27 (31)
Median of total 38 patients	39	39

Data are presented as MVD in spot 1/spot 2 (average) for each specimen.

than that of normal tissue, for a given type of tumor, we should be able to assume that a highly vascularized one comprises more oxygenated cells in a given area than a poorly vascularized one. However, little data available to date can provide direct evidence for this postulation. Study focusing on the relation of MVD and tumor virtual oxygen profile is needed to clarify this problem. MVD heterogeneity in tumors is another important issue awaiting further study. In the present study, although analyses using different groups with one of two alternative specimens yielded the same result, MVD hotspots between two specimens from the same tumor did show differing counts (Table 4). This raised the question of MVD heterogeneity between tumors and their biopsy specimens. In fact, the problem is not only about MVD. It will remain a crucial issue for pathologists to decide whether histological characteristics and molecular markers in biopsy specimen are able to represent the original tumor. Surgically treated cases should be examined in future study to analyze the differences of these factors in tumors and their biopsy specimens. In the present study, we also compared MVD in different T classifications as well as clinical stages and found there was no significant difference between each group (data not shown). Since this study only analyzed a cohort of 38 patients of which 31 patients were in stage III and stage IV, a larger cohort for investigation is needed to elucidate the relation between MVD and tumor progression.

In addition to hypoxia, radioresistance of tumor cells also influences the results of radiotherapy, and their surviving fraction at 2 Gy (SF2) has been demonstrated to be useful in comparing radiosensitivity between different tumor types (16,17). However, the results for predicting the radioresponse of an individual patient are not so convincing (1,2). In addition, low cell plating efficiency is a well-known problem that compromises its clinical application as *in vitro* assay. Several studies have assessed the predictive value of Tpot, an assay for tumor proliferative potential, but it failed to predict the outcome of radiotherapy (18,19).

In the present study, detection of several molecules in pretreatment biopsy specimens by immunohistochemical methods was found to be unrelated to local control by radiotherapy or chemoradiotherapy. The molecules tested were the proliferation marker Ki-67, the apoptosis factors p53, Bax and Bcl-2, the cell-cycle modifiers Cyclin D and CDC25B, and vascular

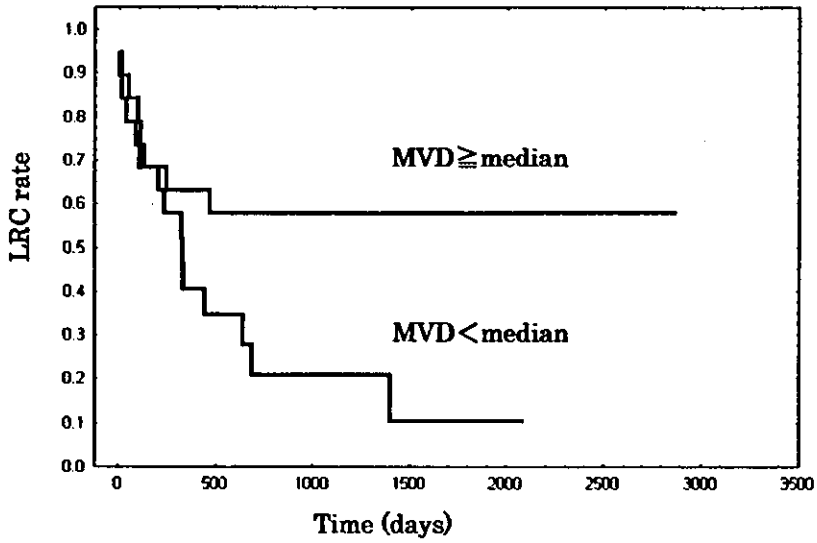

Figure 2. Kaplan–Meier analysis for local control rate for 38 hypopharyngeal cancer patients treated by radiotherapy according to MVD. Median, 39 microvessels in a ×200 high power field. $P = 0.042$.

endothelial growth factor. These findings were inconsistent with the results reported in earlier studies on head and neck cancers. However, this is not the only differing voice. The associations between the expression of these factors and tumor radiosensitivity are not well established among various studies.

Numerous reports on such clinical factors as tumor stage, T classification and N classification as prognostic factors or predictors in head and neck cancer treated by radiotherapy have yielded conflicting results. The present study showed no significant relation between tumor local control and any of the clinical factors assessed. A large cohort of patients treated by radiotherapy alone may be needed to clarify this problem. Again, because of the limited number of patients, we did not investigate whether the histological differentiation of the tumors correlated with their radioresponse.

In summary, our present study showed that the MVD of pretreated biopsy specimens may be used as a predictor for the local control of HPC treated by radiotherapy alone or chemoradiotherapy. Compared with other predictive assays, MVD count may be a simple and convenient method for clinicians to stratify patients for treatment alternatives. Nevertheless, since the vessel count is a subjective method and results may vary with the observer, we tried to determine the oxygenated area of whole biopsy specimens with an image analysis apparatus as an objective method of predicting tumor hypoxia and the outcome of radiotherapy. The results of a pioneer study on early stage laryngeal cancer are exciting and further study is in progress for its application to prediction of the radiosensitivity of HPC as well as cancers in other areas (20).

Acknowledgments

This work was supported in part by Japan–China Medical Association and Grant for Scientific Research Expenses for Health Labor and Welfare Programs, by the Foundation for the Promotion for Cancer Research, and by 2nd-Term Comprehensive 10-year Strategy for Cancer Control. We thank Dr Tomoyuki Hanaoka and Dr Takashi Sangai for their statistical assistance. We also thank Yoko Okuhara and Chie Okumura for their technical assistance.

References

1. Bjork-Eriksson T, West CM, Karlsson E, Slevin NJ, Davidson SE, James RD, et al. The in vitro radiosensitivity of human head and neck cancers. *Br J Cancer* 1998;77:2371–5.
2. Stausbol-Gron B, Overgaard J. Relationship between tumour cell in vitro radiosensitivity and clinical outcome after curative radiotherapy for squamous cell carcinoma of the head and neck. *Radiother Oncol* 1999;50:47–55.
3. Koelbl O, Rosenwald A, Haberl M, Muller J, Reuther J, Flentje M. p53 and Ki-67 as predictive markers for radiosensitivity in squamous cell carcinoma of the oral cavity? an immunohistochemical and clinicopathologic study. *Int J Radiat Oncol Biol Phys* 2001;49:147–54.
4. Miyata H, Doki Y, Shiozaki H, Inoue M, Yano M, Fujiwara Y, et al. Monden M.CDC25B and p53 are independently implicated in radiation sensitivity for human esophageal cancers. *Clin Cancer Res* 2000;6:4859–65.
5. Gallo O, Boddi V, Calzolari A, Simonetti L, Trovati M, Bianchi S. bcl-2 protein expression correlates with recurrence and survival in early stage head and neck cancer treated by radiotherapy. *Clin Cancer Res* 1996;2:261–7.
6. Homma A, Furuta Y, Oridate N, Nakano Y, Yagi K, Nagahashi T, et al. Correlation of clinicopathological parameters and biological markers related to apoptosis and proliferative activity with a clinical outcome in squamous cell carcinoma of the larynx treated with concurrent chemoradiotherapy. *Auris Nasus Larynx* 2001;28(Suppl): S87–94.
7. Shintani S, Kiyota A, Mihara M, Nakahara Y, Terakado N, Ueyama Y, et al. Association of preoperative radiation effect with tumor angiogenesis and vascular endothelial growth factor in oral squamous cell carcinoma. *Jpn J Cancer Res* 2000;91:1051–7.
8. Magne N, Pivot X, Bensadoun RJ, Guardiola E, Poissonnet G, Dassonville O, et al. The relationship of epidermal growth factor receptor levels to the prognosis of unresectable pharyngeal cancer patients treated by chemoradiotherapy. *Eur J Cancer* 2001;37:2169–77.
9. Aebersold DM, Burri P, Beer KT, Laissue J, Djonov V, Greiner RH, et al. Expression of hypoxia-inducible factor-1alpha: a novel predictive and prognostic parameter in the radiotherapy of oropharyngeal cancer. *Cancer Res* 2001;61:2911–6.

10. Vanselow B, Eble MJ, Rudat V, Wollensack P, Conradt C, Dietz A. Oxygenation of advanced head and neck cancer: prognostic marker for the response to primary radiochemotherapy. *Otolaryngol Head Neck Surg* 2000;122:856–62.
11. Rudat V, Stadler P, Becker A, Vanselow B, Dietz A, Wannenmacher M, et al. Predictive value of the tumor oxygenation by means of PO_2 histography in patients with advanced head and neck cancer. *Strahlenther Onkol* 2001; 177:462–8.
12. Kamijo T, Yokose T, Hasebe T, Yonou H, Sasaki S, Hayashi R, et al. Potential role of microvessel density in predicting radiosensitivity of T1 and T2 stage laryngeal squamous cell carcinoma treated with radiotherapy. *Clin Cancer Res* 2000;6:3159–65.
13. Vukovic V, Haugland HK, Nicklee T, Morrison AJ, Hedley DW. Hypoxia-inducible factor-1alpha is an intrinsic marker for hypoxia in cervical cancer xenografts. *Cancer Res* 2001;61:7394–8.
14. Thomlinson RH, Gray LH. The histological structure of some human lung cancers and the possible implications for radiotherapy. *Br J Cancer* 1955; 9:539–49.
15. Aebersold DM, Beer KT, Laissue J, Hug S, Kollar A, Greiner RH, et al. Intratumoral microvessel density predicts local treatment failure of radically irradiated squamous cell cancer of the oropharynx. *Int J Radiat Oncol Biol Phys* 2000;48:17–25.
16. Fertil B, Malaise EP. Inherent cellular radiosensitivity as a basic concept for human tumor radiotherapy. *Int J Radiat Oncol Biol Phys* 1981;7:621–9.
17. Deacon J, Peckham MJ, Steel GG. The radioresponsiveness of human tumours and the initial slope of the cell survival curve. *Radiother Oncol* 1984;2:317–23.
18. Hoyer M, Jorgensen K, Bundgaard T, Johansen LV, Bentzen SM, Overgaard M, et al. Lack of predictive value of potential doubling time and iododeoxyuridine labelling index in radiotherapy of squamous cell carcinoma of the head and neck. *Radiother Oncol* 1998;46:147–55.
19. Tsang RW, Wong CS, Fyles AW, Levin W, Manchul LA, Milosevic M, et al. Tumour proliferation and apoptosis in human uterine cervix carcinoma II: correlations with clinical outcome. *Radiother Oncol* 1999;50:93–101.
20. Kamijo T, Yokose T, Hasebe T, Yonou H, Hayashi R, Ebihara S, et al. Image analysis of microvessel surface area predicts radiosensitivity in early-stage laryngeal carcinoma treated with radiotherapy. *Clin Cancer Res* 2001;7:2809–14.

Int. J. Cancer: **109**, 194–199 (2004)

Publication of the International Union Against Cancer

PROMOTER HYPERMETHYLATION OF *E-CADHERIN* AND ITS ABNORMAL EXPRESSION IN EPSTEIN-BARR VIRUS-ASSOCIATED GASTRIC CARCINOMA

Makoto SUDO[1,2], Ja-Mun CHONG[1], Kazuya SAKUMA[3], Tetsuo USHIKU[1], Hiroshi UOZAKI[1], Hideo NAGAI[3], Nobuaki FUNATA[4], Yoshiro MATSUMOTO[2] and Masashi FUKAYAMA[2]*

[1]*Department of Pathology, Graduate School of Medicine, University of Tokyo, Tokyo, Japan*
[2]*First Department of Surgery, University of Yamanashi, Yamanashi, Japan*
[3]*Department of Surgery, Jichi Medical School, Tochigi, Japan*
[4]*Department of Pathology, Tokyo Metropolitan Komagome Hospital, Tokyo, Japan*

Promoter hypermethylation of various tumor-related genes is extremely frequent in Epstein-Barr virus (EBV)-associated gastric carcinoma (EBVaGC). To investigate the significance of the promoter methylation in EBVaGC, we focused on one of the important proteins in the carcinogenesis of the stomach, E-cadherin. Methylation-specific PCR analysis (MSP) was applied to surgically resected gastric carcinomas, together with immunohistochemistry, PCR-based analysis of mutations and allelic loss, and site-specific MSP of *E-cadherin* gene. By MSP, nearly all of the carcinomas showed aberrant methylation of *E-cadherin* promoter in EBVaGC (21/22), and the frequency of this aberration was significantly higher than that in EBV-negative gastric carcinoma (GC; 45/81; $p = 0.0003$). According to immunohistochemistry of E-cadherin, the frequency of abnormal staining pattern in EBVaGC (87%) was comparable to that in the diffuse type (80%), but higher than that in the intestinal type of EBV-negative GC (47%). Promoter methylation was well correlated with abnormal staining pattern in EBVaGC, but not in EBV-negative GC. Neither mutation nor allelic loss of *E-cadherin* was observed in EBVaGC. Methylation status of *E-cadherin* within each carcinoma was heterogeneous as far as examined. Thus, in addition to the known association involving p16, we determined that promoter methylation-mediated silencing of *E-cadherin* gene was also closely associated with the development of EBVaGC, although it becomes heterogeneous within a given tumor along its progression.

Key words: *Epstein-Barr virus; gastric carcinoma;* E-cadherin*; methylation*

Epstein-Barr virus (EBV)-associated gastric carcinoma (EBVaGC) is a unique type of gastric carcinoma (GC) that accounts for 5–18% of GCs reported around the world. EBV-encoded small RNA (EBER) is present in nearly all of the carcinoma cells in the intramucosal stage. EBV in EBVaGC is monoclonal by Southern blot hybridization analysis with probes adjacent to the unique terminal repeat of EBV DNA. EBVaGC also has some characteristic clinicopathologic features, such as male preference, predominant involvement of the proximal stomach, frequent accompaniment of atrophic gastritis, a moderately differentiated tubular or poorly differentiated solid type of histology[1–3] and specific expression of the splice variants of CD44 and IL-1β.[4,5] Given these many distinctions, the carcinogenic process of EBVaGC is thought to be quite different from that of EBV-negative GC.

EBV nuclear antigen 2 (EBNA2) and latent membrane protein 1 (LMP1) are latency gene products of EBV. The former is capable of immortalizing human lymphocytes, the latter capable of transforming rodent fibroblasts. Since neither is expressed in EBVaGC,[6,7] genetic or epigenetic alterations of the infected cells might be directly responsible for the development of EBVaGC. In an investigation of the genetic changes, the deletion of 5q and/or 17p and the microsatellite instability were found to be extremely rare in EBVaGC, but very frequent in EBV-negative GC.[8] On the other hand, Kang *et al.*[9] and our own group[10] recently demonstrated that promoter hypermethylation of various tumor-related genes occurs much more frequently in EBVaGC than in EBV-negative GC. The subsequent reduction of gene expression has been observed in at least one tumor suppressor gene, *p16*.[11]

In the present study, we focused on E-cadherin, another protein important in the carcinogenesis of the stomach. E-cadherin is a Ca^{2+}-dependent cell-cell adhesion molecule that plays an essential role in the formation and maintenance of the normal architecture and function of epithelial tissues.[12–14] Abnormalities of the gene and gene expression of E-cadherin have been frequently observed in gastric carcinoma,[15–20] and the germline mutation was identified in the hereditary diffuse gastric carcinoma kindred.[21] However, few studies have correlated abnormalities of E-cadherin with the EBV infection.[22] In the present study, to clarify the significance of the promoter hypermethylation of *E-cadherin* in EBVaGC, we demonstrated its clinicopathologic features and its characteristic gene expression in GC with and without EBV infection, together with the specific analyses of *E-cadherin* gene in EBVaGC, such as genetic abnormalities, and regional heterogeneity of methylation status.

MATERIAL AND METHODS

The materials consisted of 103 gastric carcinomas that had been surgically resected at Jichi Medical School or Tokyo Metropolitan Komagome Hospital from 1988 to 1998. Fresh tissues of gastric carcinoma were frozen in liquid nitrogen immediately after surgical resection and stored at −80°C until use. Histologic typing of the carcinoma and the pathology of the resected stomachs were evaluated according to the Japanese Classification of Gastric Carcinoma.[23] We also adopted Lauren's classification of gastric carcinoma,[24] intestinal and diffuse.

To determine the presence or absence of EBV, EBER *in situ* hybridization was applied to the formalin-fixed and paraffin-embedded sections as described previously.[3] Genomic DNA was isolated from the frozen tissues by a standard phenol/chloroform

Abbreviations: EBER, Epstein-Barr virus-encoded small RNA; EBV, Epstein-Barr virus; EBVaGC, Epstein-Barr virus-associated gastric carcinoma; GC, gastric carcinoma; LOH, loss of heterozygosity; MSP, methylation-specific polymerase chain reaction; PCR-SSCP, polymerase chain reaction-single-strand conformational polymorphism.

Grant sponsor: Grant-in Aid for Scientific Research on Priority Areas, Ministry of Education, Culture, Sports, Science, and Technology of Japan.

*Correspondence to: Department of Pathology, Graduate School of Medicine, University of Tokyo, 7-3-1 Hongo, Bunkyo-ku, Tokyo 113-0033, Japan. Fax: +81-3-3815-8379. E-mail: mfukayama-tky@umin.ac.jp

Received 26 May 2003; Revised 24 September 2003; Accepted 1 October 2003

DOI 10.1002/ijc.11701

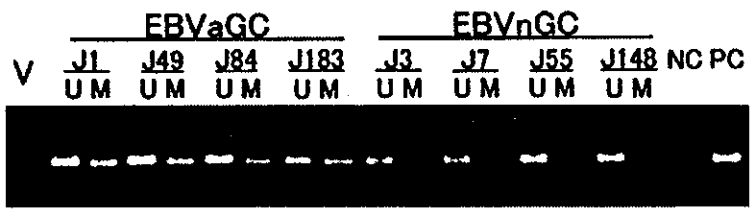

FIGURE 1 – MSP analysis of promoter hypermethylation of *E-cadherin* gene in EBV-associated and EBV-negative gastric carcinoma. Representative result of MSP of 4 EBVaGC cases (J1, J49, J84 and J183) and 4 EBV-negative GC (EBVnGC; J3, J7, J55 and J148). All 4 EBVaGC cases and 1 EBV-negative GC case (case J7) were considered methylation-positive. U, unmethylated primer set; M, methylated primer set; V, DNA marker V; NC, negative control; PC, positive control.

procedure. Due to limited sample size and relatively long duration of the tissue storage, DNA, but not RNA, could be used for the mutation analysis.

Methylation-specific polymerase chain reaction of E-cadherin gene promoter

Bisulfite modification of genomic DNA was performed[25] with the CpGenome DNA modification kit (Intergen, Purchase, NY) before the methylation-specific polymerase chain reaction (MSP) of the *E-cadherin* promoter. MSP was performed with the CpG WIZ E-cadherin Amplification kits (Intergen) according to the manufacturer's recommendation with slight modifications.[26] Reaction buffer at a final volume of 12.5 μl contained 1 unit of AmpliTaq Gold DNA polymerase (Applied Biosystems, Foster City, CA) and 1 μl of modified DNA. The temperature profiles for the amplification were as follows: initial heating at 95°C for 10 min, 40 cycles of denaturation at 95°C for 45 sec, annealing at 60°C for 45 sec and extension at 72°C for 1 min, followed by a final extension at 72°C for 10 min. A pair of positive (universal methylated and unmethylated DNA; Intergen) and negative controls (distilled water) accompanied every amplification reaction; 6 μl of each PCR product was electrophoresed in a 2% agarose gel, stained with ethidium bromide and visualized under an ultraviolet illuminator. All experiments were performed in duplicate.

Immunohistochemistry of E-cadherin

Since the high incidence of *E-cadherin* promoter hypermethylation was observed in EBVaGC, immunohistochemistry of E-cadherin was further performed to evaluate the expression of E-cadherin. For the further analysis of immunohistochemistry, the formalin-fixed and paraffin-embedded sections were available for EBVaGC when the size of the carcinoma was more than 1 cm (15 cases). For EBV-negative GCs, the specimens of Jichi Medical School were subjected to immunohistochemistry (19 intestinal and 15 diffuse type, respectively). Sections 4 μm thick were cut from formalin-fixed and paraffin-embedded specimens, deparaffinized in xylene and rehydrated in alcohol. The sections were autoclaved in 0.01 M citrate-phosphate buffer (pH 6.0) with 0.1% of Tween20 at 121°C for 10 min for antigen retrieval. The monoclonal antibody to human E-cadherin (clone HECD-1, TaKaRa, Shiga, Japan) was applied to the sections and incubated at room temperature for 1 hr. Following blockage of endogenous peroxidase activity by treatment with 0.3% hydrogen peroxide in methanol for 10 min, a standard avidin-biotin immunoperoxidase technique was used for visualization of the reactive product.[27,28] The sections were incubated with avidin-biotin complex (Vectorstain ABC kit, Vector Laboratories, Burlingame, CA), developed in 3′-3′ diaminobenzidine, counterstained with Mayer's hematoxylin for 5 min and dehydrated in alcohol prior to mounting. The epithelium of noncancerous parts within each section (if available) and/or normal colonic epithelium served as positive controls. To obtain negative controls, the primary antibodies were omitted.

For the evaluation of the immunohistochemical results, we classified the staining patterns into 3 categories according to classification recommended by Oka *et al.*[17] Tumors showing positive signal in more than 90% of tumor cells were classified as the normal type, those showing positive signal in 10–90% of tumor cells were classified as the heterogeneous type and those expressing very weak or no signal (less than 10%) were classified as the reduced type. Both reduced and heterogeneous types were considered abnormal.

TABLE I – CORRELATION BETWEEN PROMOTER HYPERMETHYLATION OF *E-CADHERIN* AND CLINICOPATHOLOGIC FACTORS IN GASTRIC CARCINOMA

Clinicopathologic factors	Promoter methylation status		*p*
	Methylated	Unmethylated	
EBV infection			
EBVaGC	21	1	0.0003
EBVnGC[a]	45	36	
Mean age	61.6 ± 14.0	64.9 ± 11.5	NS
Gender (male:female)	48:18	32:5	NS
Histology			
Intestinal	26	22	0.0502
Diffuse	40	15	
Location[b]			
Upper and middle	51	24	NS
Lower	15	13	
Depth of invasion			
Early[c]	12	5	NS
Advanced[d]	54	32	
Lymph node metastasis			
+	50	22	0.0836
–	16	15	
Lymphatic invasion			
+	60	36	NS
–	6	1	
Venous invasion			
+	58	33	NS
–	8	4	

[a]EBVnGC; EBV-negative GC.–[b]Location of tumor; upper/middle/lower third portion of the stomach. –[c]Tumor invasion within submucosa.–[d]Tumor invasion beyond muscularis propria.

PCR-single-strand conformational polymorphism analysis and loss of heterozygosity analysis of E-cadherin gene

Due to the amount of DNA available, only 11 out of the 15 EBVaGC cases examined in the immunohistochemical study were further subjected to PCR-single-strand conformational polymorphism (SSCP) and loss of heterozygosity (LOH) analyses. Exons 6–9 of *E-cadherin* gene were evaluated by PCR-SSCP analysis with subsequent sequencing of the abnormal bands. Exons 8 and 9 of the *E-cadherin* gene have been identified as the region of the mutation hot spot in diffuse-type gastric carcinoma.[29] PCR-SSCP analysis was performed according to the established protocols.[20,30] Electrophoresis was performed on 6% neutral polyacrylamide gels at 15 mA/1,500 V for 4 hr. The gels were dried and exposed to X-ray film at −80°C overnight. All experiments were performed in duplicate. MKN45, a cell line that harbors a mutation on exon 6, was used as a mutation-positive control.[30] When mobility shift SSCP bands were present, they were isolated from the gels and subjected to PCR using the same primer sets as those used in the prior PCR. The PCR products were cloned into the vector pCR II-TOPO (Invitrogen, Leek, The Netherlands). Sequencing was performed using a DYEnamic ET terminator cycle sequencing kit (Amersham Pharmacia Biotech, Uppsala, Sweden) with a DNA sequencer (Model 373A, Applied Biosystems).

The LOH study was performed using the tumor DNA and the matched DNA from the nonneoplastic mucosa. Radioactive PCR